Eur. Phys. J. C 20, 371–388 (2001)
Digital Object Identifier (DOI) 10.1007/s100520100652

THE EUROPEAN PHYSICAL JOURNAL C

# $K \to \pi\pi e^+e^-$ decays and chiral low-energy constants*

H. Pichl[1,2]

[1] INFN, Laboratori Nazionali di Frascati, P.O. Box 13, 00044 Frascati, Italy
[2] Institut für Theoretische Physik, Universität Wien, Boltzmanngasse 5, 1090 Wien, Austria

Received: 27 February 2001 /
Published online: 11 May 2001 – 

**Abstract.** The branching ratios of the measured decay $K_{\rm L} \to \pi^+\pi^-e^+e^-$ and of the still unmeasured decay $K^+ \to \pi^+\pi^0e^+e^-$ are calculated to next-to-leading order in chiral perturbation theory (CHPT). Recent experimental results are used to determine two possible values of the combination $(N_{16}^{\rm r} - N_{17})$ of weak low-energy couplings (LECs) from the $\mathcal{O}(p^4)$ chiral Lagrangian. The values obtained are compared to the predictions of theoretical approaches to weak counterterm couplings to distinguish between the two values. Using the favoured value of the combination $(N_{16}^{\rm r} - N_{17})$ and taking into account additional assumptions suggested by the considered models, one obtains the branching ratio of the second decay as a function of the unknown combination $(N_{14}^{\rm r} + 2N_{15}^{\rm r})$ of weak low-energy couplings. Finally, using values of the individual LECs derived from a particular model, one predicts the branching ratio of the $K^+$ decay.

## 1 Introduction

During the last years, there has been a lot of theoretical and experimental interest in the decay of the $K_{\rm L}$ into a pair of charged pions and a pair of leptons. This interest focused on the decay width itself [1–8] and on the possibility of constructing $CP$-violating observables [1–4, 7–12] as well as on other related topics [13,14]. From the experimental analysis of the corresponding radiative decay, it was found that the decay amplitude consists of a bremsstrahlung component and a direct emission part. The contribution due to bremsstrahlung is given via Low's theorem by the amplitude of the decay $K_{\rm L} \to \pi^+\pi^-$. This amplitude is mainly due to the $K_1^0$ admixture, which allows for this decay (indirect $CP$ violation). As a consequence, the final state of the radiative decay can be found to be in $CP$-even as well as $CP$-odd configurations. Hence, in principle, there is interference between the $CP$-conserving parts of the direct emission amplitude and the $CP$-violating bremsstrahlung amplitude. But as long as the polarization of the on-shell photon is not measured, this interference is not accessible. This is the reason why one looks directly to the decay with a lepton pair, since the angle between the two planes spanned by the pions and leptons can be used to construct a $CP$-violating observable [1–4,9,10]. In this paper, I do not focus on the $CP$-violating aspects of this decay. I calculate the decay amplitude in CHPT up to $\mathcal{O}(p^4)$ and use the most recent available data from experiments [11,15,16] (which were mostly dedicated to the study of possible $CP$-violating effects) to derive a value for the unknown combination $(N_{16}^{\rm r}(\mu) - N_{17})$ of low-energy couplings (LECs) from the weak $\mathcal{O}(p^4)$ chiral Lagrangian. Until now, theoretical predictions can only be compared to the branching ratio over the entire phase space, which makes it impossible to extract a precise value for this combination. Furthermore, it is not possible to determine this value unambiguously from experiment; therefore, one has to turn to LEC models and their predictions for low-energy couplings to find the favoured value.

Once the value of this particular combination is fixed, I use it as input together with additional assumptions about the weak LEC $N_{17}$ for the second non-leptonic decay discussed in this paper: $K^+ \to \pi^+\pi^0e^+e^-$. If we use new data from the corresponding radiative decay $K^+ \to \pi^+\pi^0\gamma$ [17], we can give the magnetic amplitude of $K^+ \to \pi^+\pi^0e^+e^-$ without any unknown parameter at $\mathcal{O}(p^4)$ and it is possible to predict the branching ratio ${\rm BR}(K^+ \to \pi^+\pi^0e^+e^-)$ as a function of the unknown combination $(N_{14}^{\rm r}(\mu) + 2N_{15}^{\rm r}(\mu))$ of weak LECs.

## 2 Effective chiral Lagrangians

Chiral perturbation theory [18,19] is the ideally suited framework to discuss these processes. It is the low-energy realization of the standard model respecting the approximate chiral symmetry of the light quark sector. In fact, the demand of invariance under chiral rotations (in our case, these are $SU(3)$ rotations) allows one to write down the most general effective Lagrangian of strong interactions amongst the light pseudoscalar meson octet. The approximate chiral symmetry $SU(3)_{\rm L} \times SU(3)_{\rm R}$ seems to be real-

* Work supported in part by TMR, EC-Contract No. ERBFMRX-CT980169 (EURODA$\Phi$NE)

ized à la Nambu–Goldstone, which means that it is spontaneously broken to the well-known $SU(3)_V$. The breakdown of the symmetry gives rise to eight almost massless would-be Goldstone bosons because there are eight broken axial generators. According to Goldstone's theorem, the quantum numbers of these particles are fixed by the quantum numbers of the broken generators; thus, one identifies the light pseudoscalars with these particles.

In the scheme of Gasser and Leutwyler [19], the most general $\mathcal{O}(p^2)$ Lagrangian including strong, electromagnetic and semileptonic weak interactions reads as follows:

$$\mathcal{L}_2 = \frac{F^2}{4}\langle D_\mu U D^\mu U^\dagger + \chi U^\dagger + \chi^\dagger U\rangle, \qquad (2.1)$$

where $D_\mu U$ is the covariant derivative with respect to external, non-propagating fields. If we specialize to the case of external photons,

$$D_\mu U = \partial_\mu U + \mathrm{i}eA_\mu[Q,U],$$
$$Q = \frac{1}{3}\cdot \mathrm{diag}(2,-1,-1), \qquad (2.2)$$

where Q is the quark charge matrix for the flavours up, down and strange. $U$ is a $3\times 3$ unitary matrix which has to be expanded to the relevant order in $\Phi$:

$$U(\Phi) = \mathrm{e}^{\mathrm{i}\sqrt{2}\Phi/F}, \qquad (2.3)$$

where the mesons are collected in the matrix $\Phi$:

$$\Phi = \begin{pmatrix} \frac{\pi^0}{\sqrt{2}} + \frac{\eta_8}{\sqrt{6}} & \pi^+ & K^+ \\ \pi^- & -\frac{\pi^0}{\sqrt{2}} + \frac{\eta_8}{\sqrt{6}} & K^0 \\ K^- & \bar{K}^0 & -2\frac{\eta_8}{\sqrt{6}} \end{pmatrix}. \qquad (2.4)$$

$F$ equals to lowest order the pion decay constant, $F_\pi = 92.4\,\mathrm{MeV}$. In general, $\chi$ contains external scalar and pseudoscalar matrix-valued fields, but here it is proportional to the quark mass matrix. In this way, explicit chiral symmetry breaking can be incorporated in the effective Lagrangians in a very elegant way:

$$\chi = 2B_0\cdot \mathrm{diag}(m_u, m_d, m_s). \qquad (2.5)$$

$B_0$ is related to the order parameter of the spontaneous breakdown of the chiral symmetry, the quark condensate. It will not appear explicitly because it can be absorbed in the squared meson masses.

For the calculation of non-leptonic kaon decays, we also need an effective Lagrangian describing the weak interactions of the mesons. This effective weak Lagrangian cannot be invariant under chiral rotations, hence chiral invariance cannot be the guideline. Starting from an effective strangeness-changing $\Delta S = 1$ four-quark Hamiltonian, one writes down a hadronically realized Lagrangian that transforms in the same way under $SU(3)_\mathrm{L}\times SU(3)_\mathrm{R}$ as this Hamiltonian. At lowest order, the needed weak Lagrangian is found to be:

$$\mathcal{L}_2^{\Delta S=1} = G_8\langle \lambda L_\mu L^\mu\rangle + G_{27}\left[L_{\mu 23}L_{11}^\mu + \frac{2}{3}L_{\mu 21}L_{13}^\mu\right] + \mathrm{h.c.}, \qquad (2.6)$$

where $\lambda = (\lambda_6 - \mathrm{i}\lambda_7)/2$ projects out the correct octet quantum numbers and $L_\mu = \mathrm{i}F^2U^\dagger D_\mu U$ is the hadronic left-chiral current in analogy to the left-chiral quark current at the level of the effective Hamiltonian. The two couplings $G_8$ and $G_{27}$ have to be obtained from experiment and the determination of these couplings involves some subtleties. In principle, the couplings are obtained from $K \to \pi\pi$ decays. Comparison of experiments with the leading-order $\mathcal{O}(p^2)$ calculations yields the "canonical" values $|G_8| \simeq 9.1\cdot 10^{-6}\,\mathrm{GeV}^{-2}$ and $G_{27}/G_8 \simeq 1/18$, where this approximate ratio of the two couplings introduces uncertainties when the 27-plet coupling enters the game. However, due to the smallness of the 27-plet coupling, one can usually neglect this part of the Lagrangian unless the octet contribution vanishes. Then also the 27-plet contribution may become important (see Sect. 3.2).

For completeness, one should remark that in [20] the relevant $K \to \pi\pi$ decays were analyzed up to $\mathcal{O}(p^4)$ and it was found that these additional corrections contribute to $G_8$ with about 30%, whereas the $G_{27}$ coupling is only modified by a few percent. Thus, if one takes into account these order $p^4$ corrections, the value of the coupling $|G_8|$ appearing in (2.6) should better be $\sim 6.4\cdot 10^{-6}\,\mathrm{GeV}^{-2}$. Throughout this work, however, I am using the canonical standard values.

The chiral Lagrangians (2.1) and (2.6) allow us to calculate tree-level amplitudes of chiral order $p^2$ and one-loop diagrams of chiral order $p^4$ which usually introduce divergences. In order to get rid of these divergences and to take into account further finite local corrections appearing at $\mathcal{O}(p^4)$, e.g. through new interactions arising from the chiral anomaly, one also has to consider the most general $\mathcal{O}(p^4)$ interaction Lagrangians.

The most general strong Lagrangian of order $p^4$, invariant under $C$, $P$ and chiral transformations, was again given by Gasser and Leutwyler [19]. There is only one term in this Lagrangian that contributes to the final results in this work:

$$\mathcal{L}_4 = -\mathrm{i}L_9\langle F_\mathrm{R}^{\mu\nu} D_\mu U D_\nu U^\dagger + F_\mathrm{L}^{\mu\nu} D_\mu U^\dagger D_\nu U\rangle. \qquad (2.7)$$

Since we are interested in external photons, the $F_{\mathrm{L,R}}^{\mu\nu}$ tensors are proportional to the ordinary electromagnetic field strength tensor:

$$F_\mathrm{L}^{\mu\nu} = -eQF^{\mu\nu} = F_\mathrm{R}^{\mu\nu}, \quad F^{\mu\nu} = \partial^\mu A^\nu - \partial^\nu A^\mu. \qquad (2.8)$$

Every new term in the strong Lagrangian of order $p^4$ is furnished with an a priori unknown low-energy coupling (LEC) [19]. Since all divergences appear as local polynomials, one can absorb the divergences of the loop amplitude in the LECs. The general structure of a LEC reads

$$L_i = L_i^\mathrm{r}(\mu) + \Gamma_i \Lambda(\mu),$$
$$\Lambda(\mu) = \frac{\mu^{d-4}}{16\pi^2}\left[\frac{1}{d-4} - \frac{1}{2}(\ln(4\pi) + 1 - \gamma_\mathrm{E})\right], \qquad (2.9)$$

where $\gamma_E = 0.5772157$ is the Euler–Mascheroni constant. This is also true for weak LECs $N_i$. The coefficients $\Gamma_i$ arise from the one-loop generating functional. Because

of the regularization procedure, the measurable couplings $L_i^{\rm r}(\mu)$ (and $N_i^{\rm r}(\mu)$) become scale dependent. In the end, this scale dependence must be compensated by the scale dependent parts of loop diagrams. One should also note that the chiral subtraction prescription differs from the usual modified MS prescription.

The new octet weak interactions are organized like this [21,22]:

$$\mathcal{L}_4^{\Delta S=1} = G_8 F^2 \sum_i N_i W_i + \text{h.c.} \tag{2.10}$$

For the non-leptonic kaon decays under consideration, only the operators $W_{14}, W_{15}, W_{16}, W_{17}$ and $W_{28}$, $W_{29}$, $W_{30}$, $W_{31}$ contribute; they are listed explicitly:

$$\begin{aligned}
W_{14} &= \mathrm{i}\langle\lambda\{F_{\rm L}^{\mu\nu} + U^\dagger F_{\rm R}^{\mu\nu} U, D_\mu U^\dagger D_\nu U\}\rangle,\\
W_{15} &= \mathrm{i}\langle\lambda D_\mu U^\dagger (U F_{\rm L}^{\mu\nu} U^\dagger + F_{\rm R}^{\mu\nu}) D_\nu U\rangle,\\
W_{16} &= \mathrm{i}\langle\lambda\{F_{\rm L}^{\mu\nu} - U^\dagger F_{\rm R}^{\mu\nu} U, D_\mu U^\dagger D_\nu U\}\rangle,\\
W_{17} &= \mathrm{i}\langle\lambda D_\mu U^\dagger (U F_{\rm L}^{\mu\nu} U^\dagger - F_{\rm R}^{\mu\nu}) D_\nu U\rangle.
\end{aligned} \tag{2.11}$$

The magnetic terms (proportional to $\epsilon_{\mu\nu\rho\sigma}$) are given by

$$\begin{aligned}
W_{28} &= \mathrm{i}\epsilon_{\mu\nu\rho\sigma}\langle\lambda D^\mu U^\dagger U\rangle\langle U^\dagger D^\nu U D^\rho U^\dagger D^\sigma U\rangle,\\
W_{29} &= 2\langle\lambda[U^\dagger \tilde F_{\rm R}^{\mu\nu} U, D_\mu U^\dagger D_\nu U]\rangle,\\
W_{30} &= \langle\lambda U^\dagger D_\mu U\rangle\langle(\tilde F_{\rm L}^{\mu\nu} + U^\dagger \tilde F_{\rm R}^{mu\nu} U) D_\nu U^\dagger U\rangle,\\
W_{31} &= \langle\lambda U^\dagger D_\mu U\rangle\langle(\tilde F_{\rm L}^{\mu\nu} - U^\dagger \tilde F_{\rm R}^{\mu\nu} U) D_\nu U^\dagger U\rangle,
\end{aligned} \tag{2.12}$$

with $\tilde F_{\rm L,R}^{\mu\nu}$ the dual tensor of (2.8), $\tilde F_{\rm L,R}^{\mu\nu} = \epsilon^{\mu\nu\rho\sigma} F_{\rho\sigma\,\rm L,R}$.

Finally, we introduce a Lagrangian that embodies contributions from reducible diagrams with a WZW vertex and an $\mathcal{O}(p^2)$ $\Delta S = 1$ vertex. It only contributes to the $K^+$ decay and is given by [23–25]

$$\mathcal{L}_{an}^{\Delta S=1} = \frac{\mathrm{i}eG_8}{8\pi^2 F} \tilde F^{\mu\nu} \partial_\mu \pi^0 K^+ \overset{\leftrightarrow}{D}_\nu \pi^-, \tag{2.13}$$

where $\tilde F^{\mu\nu}$ is the dual of the ordinary electromagnetic field strength tensor (2.8), $\tilde F^{\mu\nu} = \epsilon^{\mu\nu\rho\sigma} F_{\rho\sigma}$, and the covariant derivative is the usual QED derivative.

## 3 Amplitudes

For both decays, the general form of the invariant amplitude due to covariance is

$$\mathcal{A} = \frac{e}{q^2} V_\mu \bar u(k_-)\gamma^\mu v(k_+), \tag{3.1}$$

where $q = k_- + k_+$ is the momentum of the virtual photon, $k_-$ and $k_+$ are the momenta of the electron and positron, respectively. $\mathrm{i}V_\mu$ is the generic weak $K\pi\pi(\gamma^\star)$ vertex, calculated in CHPT. It is decomposed in an electric and a magnetic part:

$$V_\mu = \mathcal{F}_1 p_{1\mu} + \mathcal{F}_2 p_{2\mu} + \mathcal{M}\epsilon_{\mu\nu\rho\sigma} p_1^\nu p_2^\rho q^\sigma, \tag{3.2}$$

where $p_1$ and $p_2$ are the outgoing momenta of the $\pi^+$ and $\pi^-(\pi^0)$ and $\mathcal{F}_1$, $\mathcal{F}_2$, $\mathcal{M}$ are form factors containing the dynamics of the two processes. A separate term proportional to the photon momentum vanishes because of the Dirac equation. The form factors are either constants or scalar functions of various products of the involved momenta.

### 3.1 $K_{\rm L} \to \pi^+\pi^-\gamma^\star$ amplitudes

This decay had already been considered in the framework of CHPT in [3]. The authors of [3] used a different basis of counterterms (this change of basis is only valid as long as one is only interested in photons in (2.2)) and a different approximation of the magnetic part of the amplitude not taking into account any energy dependence. The present calculation considers this energy dependent part [11], too, and additionally serves as a check on the results in [3].

For this decay, I assume strong isospin conservation, i.e. the up and the down quark have equal masses. Hence, the Gell-Mann–Okubo mass relation holds and we only have to deal with two independent masses: $3m_{\eta_8}^2 = 4m_K^2 - m_\pi^2$. It will be used to simplify parts of the one-loop amplitude given in the appendix.

In this paper, I use the following definitions: $K_{\rm L} = K_2^0 + \epsilon K_1^0$, where $CP|K_1^0\rangle = +|K_1^0\rangle$ and $CP|K_2^0\rangle = -|K_2^0\rangle$. $K_1^0$ and $K_2^0$ are related to the strangeness eigenstates $K^0$ and $\bar K^0$ through the following expressions:

$$\begin{aligned}
K_1^0 &= \frac{1}{\sqrt{2}}(K^0 - \bar K^0),\\
K_2^0 &= \frac{1}{\sqrt{2}}(K^0 + \bar K^0).
\end{aligned} \tag{3.3}$$

The tree-level amplitude is entirely due to the $K_1^0$ admixture, since we do not consider direct sources of $CP$ violation. In any case, the tree-level contribution is rather suppressed, especially when compared to the $K^+$ decay (Sect. 3.2). From Fig. 1 one obtains the following tree-level form factors:

$$\begin{aligned}
\mathcal{F}_1^{\rm Lt} &= -\mathrm{i}\epsilon \frac{4eG_8F}{2qp_1 + q^2}(m_K^2 - m_\pi^2),\\
\mathcal{F}_2^{\rm Lt} &= \mathrm{i}\epsilon \frac{4eG_8F}{2qp_2 + q^2}(m_K^2 - m_\pi^2),
\end{aligned} \tag{3.4}$$

where $\epsilon \simeq 2.27 \cdot 10^{-3} \mathrm{e}^{\mathrm{i}44^\circ}$ is the parameter of indirect $CP$ violation. In the remainder of the paper, we do not take into account $\mathcal{O}(p^4)$ corrections proportional to $\epsilon$ to the electric form factors. As mentioned in Sect. 2, a value of $|G_8| \simeq 9.1 \cdot 10^{-6}\,\mathrm{GeV}^{-2}$ already amounts to some $\mathcal{O}(p^4)$ contributions.

The magnetic form factor can only arise through the four weak counterterms $W_{28}, \ldots, W_{31}$ and it is in fact a result of the chiral anomaly. It is necessarily finite and does not have any energy dependence at this order. CHPT generates the following direct emission magnetic form factor:

$$\begin{aligned}
\mathcal{M}^{\rm L} &= \frac{-16eG_8}{F}(N_{29} + N_{31})\\
&= \frac{-eG_8}{2\pi^2 F}(a_2 + 2a_4),
\end{aligned} \tag{3.5}$$

where I have used the "magnetic" notation of [24,25]. These magnetic LECs are also still unknown. Experiments exhibit a large sensitivity of the magnetic amplitude to the energy of the emitted photon; therefore, I will use the experimental results of [11] (rather than the old results of

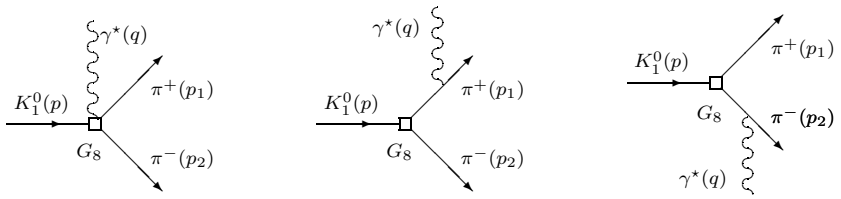


**Fig. 1.** Tree-level diagrams for $K_{\rm L} \to \pi^+\pi^-\gamma^\star$. At tree level, the $K_{\rm L}$ transition is entirely due to $K_1^0$ admixture

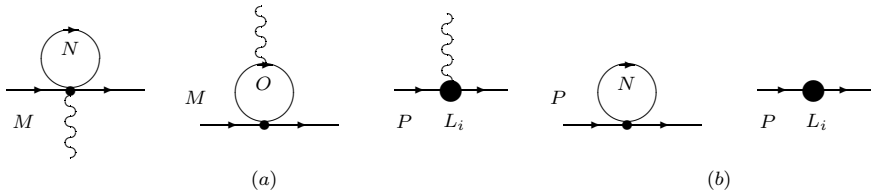


**Fig. 2a,b.** Strong insertions. **a** Loops, where the photon is emitted at the vertex or by a charged meson in the loop, and the generic photon emitting counterterm proportional to $L_i$. $M$ denotes $K_2^0$, $\pi^+$ or $\pi^-$. $N$ denotes the allowed particles in the loop: $\pi^0$, $\pi^+$, $K^+$, $\eta_8$, $K_1^0$ or $K_2^0$. $O$ denotes any charged pseudoscalar. $P$ denotes $\pi^+$ or $\pi^-$. **b** Generic loop and generic counterterm vertex proportional to $L_i$ without a photon

the experiment by Ramberg et al., [26]) to estimate the magnetic contribution. The authors of [11] use the papers by Sehgal et al. [1,2] as the theoretical background to model their Monte Carlo, but additionally introduce an energy dependence in the magnetic amplitude through a form factor that involves a kind of a $\rho$ propagator:

$$\mathcal{M}^{\rm L} = e|f_s|\frac{\tilde{g}_{M1}}{m_K^4}\mathcal{W},$$
$$\mathcal{W} = \left[1 + \frac{a_1/a_2}{(m_\rho^2 - m_K^2) + 2m_K E_\gamma^\star}\right]. \qquad (3.6)$$

Ansatz (3.6) cannot be compared directly to the magnetic form factor in [1–4,9]. Consequently according to [11], one should identify the average of $\tilde{g}_{M1}\mathcal{W}$ over the allowed range of $E_\gamma^\star$, the energy of the virtual photon, with the original magnetic coupling used in [1–4,9]. $|f_s| \simeq 3.9 \cdot 10^{-4}\,$MeV is the absolute value of the decay amplitude of $K_S \to \pi^+\pi^-$, and the experiment [11] gave for the magnetic coupling $|\tilde{g}_{M1}| = 1.35^{+0.20}_{-0.17}(\text{stat.}) \pm 0.04(\text{syst.})$ and for $a_1/a_2 = -0.720 \pm 0.028(\text{stat.}) \pm 0.009(\text{syst.})\,\text{GeV}^2$. ($a_2$ in the fraction above is not the same as the LEC $a_2$ in (3.5).) These numbers were obtained from the entire KTeV 1997 data set of more than 1811 events above background [11]. In fact, it is also this data set and this parameterization that were used to extract the most recent value of the branching ratio of $K_{\rm L} \to \pi^+\pi^-e^+e^-$ [15,16]. Additionally, the fraction $a_1/a_2$ was found from the corresponding radiative decay $K_{\rm L} \to \pi^+\pi^-\gamma$ to be $-0.729 \pm 0.026(\text{stat.}) \pm 0.015(\text{syst.})\,\text{GeV}^2$ [12], which is clearly in perfect agreement. The errors of these quantities are the sources of by far the most important contributions to the uncertainties in the extraction of the LEC combination $(N_{16}^{\rm r}(\mu) - N_{17})$.

The electric form factors at $\mathcal{O}(p^4)$ show the pleasant feature that one can obtain the form factor $\mathcal{F}_2^{\rm L}$ from the expression for $\mathcal{F}_1^{\rm L}$ by simply exchanging the pion momenta $p_1$ and $p_2$. At this order, there is no change of sign as at the tree level (3.4), since we concentrate on the $CP$-conserving part of the decay.

We begin the discussion of next-to-leading-order electric form factors by considering strong loops and strong counterterm contributions. The starting point for our analysis is the collection of diagrams in Fig. 1, where one replaces $K_1^0$ with $K_2^0$. Wave function renormalization graphs will be neglected, since the tree-level amplitude of $K_2^0 \to \pi^+\pi^-\gamma^\star$ vanishes.

Removing the photon in the left diagram of Fig. 1 and replacing the external kaon line with the appropriate loop diagrams from Fig. 2a, one obtains diagrams that are found to vanish. This feature is due to the structure of the weak $K_2^0\pi^+\pi^-$ vertex. Appropriate replacement of the kaon line in Fig. 1 with the loop diagrams drawn in Fig. 3, however, yields a finite $K_1^0$ propagator contribution to the electric form factors. The contribution must be finite, since there are no counterterms to compensate a divergence. This kind of diagrams was already considered in [1,2] and the sum of the diagrams yields

$$\mathcal{F}_{11}^{\rm Ll} = \frac{-{\rm i}eG_8}{(d-1)F}\frac{1}{[(p_1+p_2)^2 - m_K^2]}(m_\pi^2 + 2p_1p_2)$$
$$\times \{B(q^2, m_\pi^2, m_\pi^2)(4m_\pi^2 - q^2) + (4-2d)A(m_\pi^2)$$
$$- B(q^2, m_K^2, m_K^2)(4m_K^2 - q^2) - (4-2d)A(m_K^2)\}. \qquad (3.7)$$

A second kind of strong $\mathcal{O}(p^4)$ corrections is obtained from the two remaining bremsstrahlung graphs in Fig. 1 in two ways: first, by either putting the loop diagram (without photon) of Fig. 2b or the counterterm insertion (without photon) of Fig. 2b instead of the internal pion lines; and secondly, by replacing the scalar QED vertices with the diagrams of Fig. 2a. Focusing on the counterterms first, one finds that counterterms proportional to the LECs $L_4$, $L_5$ and $L_9$ from the order $p^4$ Lagrangian [19] are allowed to contribute. Calculating the sum of all the diagrams of the second kind, however, one discovers that only the con-

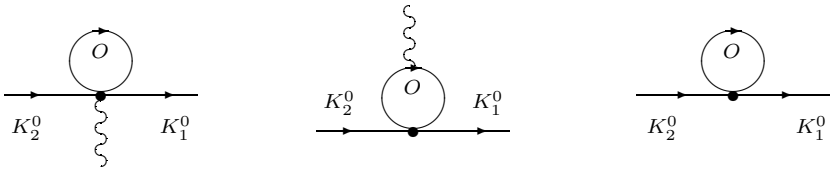


**Fig. 3.** Strong loop insertions for the external $K_2^0$ line that generate a $K_1^0$ propagator. The contributions derived from these insertions, however, are finite. $O$ denotes a charged pion or kaon

tribution from the counterterm (2.7) proportional to $L_9$ survives. The final correction of strong order $p^4$ diagrams of the second kind to the form factors is given by a very condensed and compact result:

$$\mathcal{F}_{12}^{\rm Ll} = \frac{-{\rm i}eG_8}{F}\left\{-4q^2L_9 - \frac{d-2}{d-1}[2A(m_\pi^2)+A(m_K^2)] + \frac{1}{d-1}\left[(4m_\pi^2-q^2)B(q^2,m_\pi^2,m_\pi^2) + \frac{1}{2}(4m_K^2-q^2)B(q^2,m_K^2,m_K^2)\right]\right\}. \quad (3.8)$$

The tadpole integral $A(m^2)$ and $B(p^2,m^2,m^2)$, the scalar two-propagator integral, are defined in Appendix A. $d$ is the spacetime dimension coming from dimensional regularization.

Actually, the form factor $F_{12}^{\rm Ll}$ contains divergences stemming from the functions $A$ and $B$ which are removed by the divergent part of the strong counterterm coupling $L_9$ (coming from Fig. 2a). In the finite amplitude with strong $\mathcal{O}(p^4)$ insertions, the measurable part of $L_9$ shows up: $L_9^{\rm r}(m_\rho) = (6.9 \pm 0.7)\cdot 10^{-3}$ [19]. Throughout this paper, I always choose $\mu = m_\rho$ as renormalization scale.

Weak counterterms only contribute through a diagram obtained from the direct emission diagram in Fig. 1 by replacing $K_1^0$ with $K_2^0$ and putting in the counterterm vertex from (2.10) and (2.11) instead of the lowest-order vertex. All occuring divergences from weak loop diagrams must be removed by this local counterterm contribution. The weak counterterms produce the following contribution to the electric form factors:

$$\mathcal{F}_{13}^{\rm Ll} = \frac{2{\rm i}eG_8}{3F}q^2[N_{14}-N_{15}-3(N_{16}-N_{17})], \quad (3.9)$$

where all renormalized LECs $N_i^{\rm r}$ (compare with (2.9)) depend on a scale $\mu = m_\rho$. Since the coefficient $\Gamma_{17}$ is found to vanish, the LEC $N_{17}$ is independent of the renormalization scale. The renormalized parts of the low-energy couplings enter into the amplitude of the decay, therefore it is important to know their finite values.

The combination $(N_{14}^{\rm r}-N_{15}^{\rm r})$ also appears in the counterterm part of the form factor describing the decay $K^+ \to \pi^+e^+e^-$ within the expression [27]

$$w_+ = \frac{64\pi^2}{3}[N_{14}^{\rm r}(\mu)-N_{15}^{\rm r}(\mu)+3L_9^{\rm r}(\mu)] + \frac{1}{3}\ln\left[\frac{\mu^2}{m_K m_\pi}\right]. \quad (3.10)$$

Old experiments [28] fixed $w_+$ at $0.89^{+0.24}_{-0.14}$, which corresponds to a value of $(N_{14}^{\rm r}(m_\rho)-N_{15}^{\rm r}(m_\rho)) \simeq -0.02$. A more refined theoretical analysis of this decay also took into account $\mathcal{O}(p^6)$ corrections to the form factor [29]. The polynomial part of this form factor is given by $W_+^{\rm pol} = G_F m_K^2(a_+ + b_+ z)$, where $z = q^2/m_K^2$ and $q$ is the momentum of the intermediate photon that gives rise to the lepton pair. The new parameter $a_+$ contains in principle also $\mathcal{O}(p^6)$ corrections and it is related with the usual $w_+$ through [29]

$$a_+ = \frac{G_8}{G_F}\left[\frac{1}{3}-w_+\right]. \quad (3.11)$$

A new experimental analysis of this decay [30] measured the parameters of the $K^+ \to \pi^+e^+e^-$ form factor and found $a_+ = -0.587 \pm 0.010$. With this new number we determine $w_+$ to be 1.086 and $(N_{14}^{\rm r}(\mu)-N_{15}^{\rm r}(\mu)) = -0.019 \pm 0.002$ at the scale $m_\rho$. One finds that the new and the old value are almost the same.

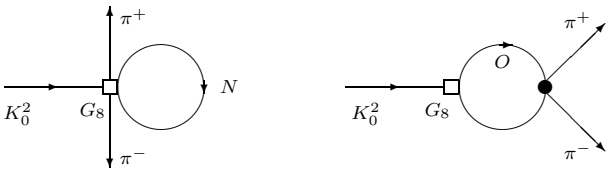


**Fig. 4.** Weak loop diagrams: the basic tadpole diagram (left) and the basic diagram of topology 1 (right). $N$ and $O$ denote the same particles as in Fig. 2

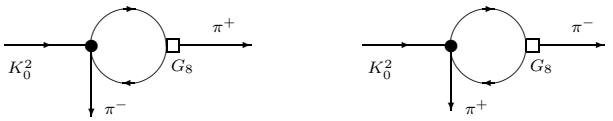


**Fig. 5.** Weak loop diagrams: the basic diagram of topology 2 (left), the basic diagram of topology 3 (right)

The contributions of weak loop graphs to the form factors are quite involved. To make it more transparent how the corrections from different kinds of weak loop graphs enter into the form factors, I present the possible kinds of diagrams in Figs. 4 and 5 and quote the results separately.

All weak tadpole diagrams can be obtained from the basic diagram (left) in Fig. 4 by appending a photon on all charged lines and on the weak vertex. It turns out that only intermediate charged particles produce non-vanishing diagrams. The tadpole part of the form factor looks very simple and reads

$$\mathcal{F}_{14}^{\rm Ll} = \frac{-2{\rm i}eG_8}{3F}\frac{1}{d-1}\{2A(m_\pi^2)(2d-4) + 2B(q^2,m_\pi^2,m_\pi^2)(q^2-4m_\pi^2)+A(m_K^2)(2d-4) + B(q^2,m_K^2,m_K^2)(q^2-4m_K^2)\}. \quad (3.12)$$

Diagrams which can be constructed from the second diagram (right) in Fig. 4 are referred to as diagrams of topology 1. Again, one has to append a photon on all charged lines as well as on the strong and weak vertex. This time, only pairs of charged pions or charged kaons may occur in the loop. The contribution of topology 1 to the form factors is found to be very compact, too, and it is given by

$$\begin{aligned}\mathcal{F}_{15}^{\mathrm{Ll}} = {} & \frac{-\mathrm{i}eG_8}{3F}\frac{1}{d-1}\left\{2(2-d)A(m_\pi^2)\right. \\ & - B(q^2,m_\pi^2,m_\pi^2)(q^2-4m_\pi^2) + (2-d)A(m_K^2) \\ & \left. - \frac{1}{2}B(q^2,m_K^2,m_K^2)(q^2-4m_K^2)\right\}. \end{aligned} \tag{3.13}$$

The diagrams considered so far produce form factors that are symmetric in the pion momenta $p_1$ and $p_2$. Besides, apart from $A$ functions only $B(q^2,m^2,m^2)$ occurs and one can easily check that all these contributions vanish for an on-shell photon.

The decay amplitude is completed with the contributions from diagrams belonging to topologies 2 and 3. These diagrams are obtained from the basic graphs in Fig. 5 through the same steps as before. The expressions that one obtains from these graphs are rather involved, thus I will not present the results explicitly in terms of the standard scalar loop functions $A$, $B$, $C$ defined in Appendix A. It is the contributions of these diagrams that introduce the asymmetry in $p_1$ and $p_2$ in the $\mathcal{O}(p^4)$ form factors. The possible pairs of particles in the loop are $(\pi^0,K^-)$, $(\eta_8,K^-)$, $(K_1^0,\pi^-)$ and $(K_2^0,\pi^-)$ for topology 2. The particles for topology 3 are the corresponding charge conjugated ones. It turns out that the diagrams with the internal combination $(K_2^0,\pi^-)$ vanish. The contributions from the other possible combinations to the form factor $\mathcal{F}_1^{\mathrm{L}}$ are given in $\mathcal{F}_{16}^{\mathrm{Ll}}$ in Appendix B; see (B.1).

By extracting only the explicit poles of the total loop contribution, one finds that all divergences are proportional to $q^2$, which corresponds to the counterterm parts of expressions (3.8) and (3.9). Furthermore, this shows that the loop amplitude of the corresponding radiative decay is finite [23,25]. Finally, the complete form factor $\mathcal{F}_1^{\mathrm{L}}$ is given by

$$\mathcal{F}_1^{\mathrm{L}} = \mathcal{F}_1^{\mathrm{Lt}} + \mathcal{F}_{11}^{\mathrm{Ll}} + \mathcal{F}_{12}^{\mathrm{Ll}} + \mathcal{F}_{13}^{\mathrm{Ll}} + \mathcal{F}_{14}^{\mathrm{Ll}} + \mathcal{F}_{15}^{\mathrm{Ll}} + \mathcal{F}_{16}^{\mathrm{Ll}}. \tag{3.14}$$

As already stated, the corresponding form factor $\mathcal{F}_2^{\mathrm{L}}$ is obtained from $\mathcal{F}_1^{\mathrm{L}}$ through the substitution $p_1 \leftrightarrow p_2$.

### 3.2 $K^+ \to \pi^+\pi^0\gamma^\star$ amplitudes

The general structure of the amplitude stays the same as in (3.1), but there is no symmetry relation between the electric form factors anymore. $p_1$ is now the momentum of the $\pi^+$ and $p_2$ the momentum of the $\pi^0$, respectively. In the limit of isospin symmetry, the octet tree-level amplitude vanishes, hence we relax the approximation of equal masses of charged and neutral pions at the tree level and take the 27-plet coupling into account, too. As already anticipated in Sect. 2, throughout the following analysis we will use again the canonical values of $|G_8|$ and $G_{27}/G_8$ which are derived from the tree level.

The tree-level form factors arise from the corresponding diagrams in Fig. 1, where one replaces $K_1^0$ with $K^+$ and $\pi^-$ with $\pi^0$ and puts the photon into the right places. In addition, the corresponding tree-level contributions with the weak coupling constant $G_{27}$ will be regarded, too. Terms proportional to $G_8$ are clearly suppressed because of approximate isospin symmetry; thus, the actual value of $G_8$ is not of too much importance for the tree level. The lowest-order amplitude reads

$$\begin{aligned}\mathcal{F}_1^{+t} = {} & 2\mathrm{i}eG_8F(m_{\pi^+}^2 - m_{\pi^0}^2)\left\{\frac{1}{2qp_1+q^2} + \frac{1}{q^2-2qp}\right\} \\ & + \frac{2\mathrm{i}eG_{27}F}{3}(5m_{K^+}^2 - 7m_{\pi^+}^2 + 2m_{\pi^0}^2) \\ & \times \frac{2qp_2}{(q^2+2qp_1)(q^2-2qp)}, \\ \mathcal{F}_2^{+t} = {} & \frac{2\mathrm{i}eF}{q^2-2qp}\left[G_8(m_{\pi^+}^2 - m_{\pi^0}^2)\right. \\ & \left. - \frac{2G_{27}}{3}(5m_{K^+}^2 - 7m_{\pi^+}^2 + 2m_{\pi^0}^2)\right]. \end{aligned} \tag{3.15}$$

The magnetic form factor at lowest order ($\mathcal{O}(p^4)$) is derived from the Lagrangian (2.10) with the counterterms in (2.12) and the WZW Lagrangian (2.13). It is necessarily finite and one calculates

$$\mathcal{M}^+ = \frac{eG_8}{4\pi^2F}(2 - 3a_2 + 6a_3), \tag{3.16}$$

where the 2 comes from the Lagrangian (2.13). Again, the values of these magnetic LECs are unknown, but comparison with the corresponding radiative $K^+$ decay [24, 25] shows that the magnetic form factor $\mathcal{M}^+$ also appears there. This suggests the use of results from the E787 experiment [17] to estimate the combination of LECs in (3.16). In this experiment on the corresponding radiative $K^+$ decay, a branching ratio from direct emission $\mathrm{BR}(K^+ \to \pi^+\pi^0\gamma; \mathrm{DE}, 55\,\mathrm{MeV} < T_{\pi^+} < 90\,\mathrm{MeV}) = [4.7 \pm 0.8(\mathrm{stat.}) \pm 0.3(\mathrm{syst.})] \cdot 10^{-6}$ is reported. Under the rather reasonable assumption that direct emission is entirely due to the magnetic amplitude, one can extract a value for the whole combination of LECs in (3.16). Of course, this does not take into account energy dependent corrections, but this is at the moment the best one can do. Moreover, the experimental data seem to indicate that neglect of energy dependent higher-order terms does not do much harm to the magnetic amplitude. The authors also find no evidence for any electric direct emission in the decay [17]. The combination of magnetic LECs in (3.16) can be extracted from the radiative decay ($q^2 = 0$) by using $\mathcal{A}(K^+ \to \pi^+\pi^0\gamma, DE) = \mathcal{M}^+\epsilon^{\mu\nu\rho\sigma}p_{1\nu}p_{2\rho}q_\sigma\epsilon_\mu^\star(q)$:

$$|2 - 3a_2 + 6a_3| = |A_4| = 2.26 \pm 0.25. \tag{3.17}$$

Turning to next-to-leading-order corrections to the electric form factors, I start again with the discussion of contributions from strong loops and strong counterterm diagrams.

From now on, strong isospin is conserved and 27-plet corrections are neglected.

Similar to the analysis in Sect. 3.1, diagrams with strong loops and strong counterterm vertices are obtained from insertions of loops and vertices in propagators or external lines in $K^+ \to \pi^+\pi^0\gamma^\star$ tree-level diagrams derived from the graphs in Fig. 1 by replacing $K_1^0 \to K^+$ and $\pi^- \to \pi^0$. Wave function renormalization diagrams are not considered because the tree-level octet amplitude for $K^+ \to \pi^+\pi^0\gamma^\star$ vanishes in the isospin limit. The necessary insertions are obtained from the diagrams in Fig. 2, where $M$ denotes this time $K^+$, $\pi^+$ or $\pi^0$ and $N$ denotes $\pi^+$, $\pi^0$, $K^+$, $K^0$, $\bar{K}^0$ or $\eta_8$, respectively. Here, $P$ denotes $K^+$ or $\pi^+$. Introducing equivalent replacements as in Sect. 3.1 one obtains the strong corrections to the next-to-leading-order form factors given by

$$\begin{aligned}
\mathcal{F}_{11}^{+\mathrm{l}} &= \frac{-\mathrm{i}eG_8}{F}\left\{-4q^2L_9 - \frac{d-2}{d-1}[2A(m_\pi^2)+A(m_K^2)]\right.\\
&\quad + \frac{1}{d-1}\left[(4m_\pi^2-q^2)B(q^2,m_\pi^2,m_\pi^2)\right.\\
&\quad \left.\left. + \frac{1}{2}(4m_K^2-q^2)B(q^2,m_K^2,m_K^2)\right]\right\},\\
\mathcal{F}_{21}^{+\mathrm{l}} &= 0. \qquad (3.18)
\end{aligned}$$

The vanishing of $\mathcal{F}_{21}^{+\mathrm{l}}$ is related to C invariance of the strong Lagrangian. Although counterterms proportional to $L_4$, $L_5$ and $L_9$ are allowed to contribute, only the $L_9$ term (2.7) survives the summation of all contributions. The divergent part of the LEC $L_9$ removes the divergences of the result in (3.18). The form factor $\mathcal{F}_{11}^{+\mathrm{l}}$ vanishes in the limit of an on-shell photon.

Substituting the relevant weak counterterm vertex from (2.10) and (2.11) for the lowest-order vertex in the direct emission diagram in Fig. 1 and making the necessary particle replacements, one calculates this local contribution to the form factors:

$$\begin{aligned}
\mathcal{F}_{12}^{+\mathrm{l}} &= \frac{-\mathrm{i}eG_8}{3F}[-6qp_2(N_{14}-N_{15}-N_{16}-N_{17})\\
&\quad - 4q^2(N_{14}-N_{15})],\\
\mathcal{F}_{22}^{+\mathrm{l}} &= \frac{-\mathrm{i}eG_8}{3F}[6qp_1(N_{14}-N_{15}-N_{16}-N_{17})\\
&\quad - 2q^2(N_{14}+2N_{15}) + 6q^2(N_{16}-N_{17})]. \qquad (3.19)
\end{aligned}$$

One recovers the finite combination $(N_{14}-N_{15}-N_{16}-N_{17})$ of the corresponding radiative decay and the structure that is governed by gauge invariance [23,25]. Divergences arising from weak loop diagrams are removed by the combinations of LECs proportional to $q^2$ in (3.19). Using the determined value of $(N_{16}^{\mathrm{r}}-N_{17})$ and appealing to some models for weak low-energy couplings, the whole finite decay amplitude contains in the end only the unknown combination $(N_{14}^{\mathrm{r}}+2N_{15}^{\mathrm{r}})$ from the form factor $\mathcal{F}_{22}^{+\mathrm{l}}$ in (3.19). I will come back to this later. At this point, it should be mentioned that a similar combination of the same weak LECs, namely $(2N_{14}^{\mathrm{r}}+N_{15}^{\mathrm{r}})$, appears in the decay $K_{\mathrm{L}} \to \pi^0\pi^0\gamma^\star$ considered in [31].

Weak tadpole diagrams can be constructed from the basic diagram in Fig. 4 (with $K_2^0 \to K^+$, $\pi^- \to \pi^0$) by following the same procedure as in Sect. 3.1 and one obtains

$$\begin{aligned}
\mathcal{F}_{13}^{+\mathrm{l}} &= \frac{-\mathrm{i}eG_8}{3F}\frac{1}{d-1}\{(2d-4)[A(m_\pi^2)+A(m_K^2)]\\
&\quad + B(q^2,m_\pi^2,m_\pi^2)(q^2-4m_\pi^2)\\
&\quad + B(q^2,m_K^2,m_K^2)(q^2-4m_K^2)\},\\
\mathcal{F}_{23}^{+\mathrm{l}} &= \frac{-\mathrm{i}eG_8}{3F}\frac{1}{d-1}\{(2d-4)[A(m_\pi^2)-A(m_K^2)]\\
&\quad + B(q^2,m_\pi^2,m_\pi^2)(q^2-4m_\pi^2)\\
&\quad - B(q^2,m_K^2,m_K^2)(q^2-4m_K^2)\}. \qquad (3.20)
\end{aligned}$$

One finds that $\eta_8$ loops do not contribute. In case of an on-shell photon, the expressions (3.20) vanish.

Diagrams of the topology 1 are constructed from the right diagram in Fig. 4 (with $K_2^0 \to K^+$, $\pi^- \to \pi^0$) replacing the charged meson pairs in the loop with $(\pi^+,\pi^0)$, $(K^+,\bar{K}^0)$, or with $(\pi^+,\eta_8)$ (in an appropriate momentum convention). The last combination of intermediate particles vanishes in the isospin limit. Appending a photon where it is possible and summing up the diagrams, one finds a compact result involving only $A$ and $B(q^2,m^2,m^2)$:

$$\begin{aligned}
\mathcal{F}_{14}^{+\mathrm{l}} &= \frac{-\mathrm{i}eG_8}{F(d-1)}\left\{(d-2)\left[A(m_K^2)+\frac{4}{3}A(m_\pi^2)\right]\right.\\
&\quad + \frac{1}{2}B(q^2,m_K^2,m_K^2)(q^2-4m_K^2)\\
&\quad \left. + \frac{2}{3}B(q^2,m_\pi^2,m_\pi^2)(q^2-4m_\pi^2)\right\},\\
\mathcal{F}_{24}^{+\mathrm{l}} &= \frac{-\mathrm{i}eG_8}{F(d-1)}\left\{(2-d)\left[A(m_K^2)+\frac{2}{3}A(m_\pi^2)\right]\right.\\
&\quad + \frac{1}{2}B(q^2,m_K^2,m_K^2)(4m_K^2-q^2)\\
&\quad \left. + \frac{1}{3}B(q^2,m_\pi^2,m_\pi^2)(4m_\pi^2-q^2)\right\}. \qquad (3.21)
\end{aligned}$$

Expressions (3.21) vanish in the on-shell limit and their divergences are clearly proportional to $q^2$. The last and by far most voluminous contributions to the electric $\mathcal{O}(p^4)$ form factors come from diagrams of the topologies 2 and 3 which can be derived from the basic diagrams in Fig. 5 as before. Possible virtual pairs are $(\pi^0,K^-)$, $(\eta_8,K^-)$, $(K^0,\pi^-)$ and $(K^0,\pi^0)$, $(K^0,\eta_8)$, $(K^+,\pi^+)$, respectively. The obtained results, labelled as $\mathcal{F}_{15,25}^{+\mathrm{l}}$ and $\mathcal{F}_{16,26}^{+\mathrm{l}}$, are listed in Appendix C, (C.1), (C.2) and (C.3), (C.4). The complete form factor $\mathcal{F}_1^+$ is finally given by

$$\mathcal{F}_1^+ = \mathcal{F}_1^{+t} + \mathcal{F}_{11}^{+\mathrm{l}} + \mathcal{F}_{12}^{+\mathrm{l}} + \mathcal{F}_{13}^{+\mathrm{l}} + \mathcal{F}_{14}^{+\mathrm{l}} + \mathcal{F}_{15}^{+\mathrm{l}} + \mathcal{F}_{16}^{+\mathrm{l}}. \quad (3.22)$$

$\mathcal{F}_2^+$ is obtained from the corresponding sum.

## 4 Numerical analysis

### 4.1 Decay width

The decay width for the processes in question is given by the following standard formula:

$$\Gamma(K \to \pi_1\pi_2 e^+e^-) = \frac{m_e^2}{128\pi^8 m_K} \times \int \frac{\mathrm{d}^3p_1}{2E_1}\frac{\mathrm{d}^3p_2}{2E_2}\frac{\mathrm{d}^3k_+}{2E_+}\frac{\mathrm{d}^3k_-}{2E_-}\delta^{(4)}(p_f - p_i)\sum_{\text{spins}}|\mathcal{A}|^2, \tag{4.1}$$

where $p_1$ is always the momentum of the positive pion and $p_2$ refers to the corresponding other pion, $\pi^-$ or $\pi^0$. As usual, $p_{i,f}$ denote the sums of ingoing and outgoing momenta, respectively. In fact, $p_i^\mu = (m_K, 0, 0, 0)$. The squared transition amplitude for both decays in question reads as follows:

$$\begin{aligned}
\sum_{\text{spins}}|\mathcal{A}|^2 = {} & \frac{e^2}{m_e^2q^4}\{-(m_e^2 + k_+k_-)[|\mathcal{F}_1|^2p_1^2 + |\mathcal{F}_2|^2p_2^2 \\
& + p_1p_2(\mathcal{F}_1\mathcal{F}_2^\star + \mathcal{F}_1^\star\mathcal{F}_2)] + 2|\mathcal{F}_1|^2k_+p_1k_-p_1 \\
& + 2|\mathcal{F}_2|^2k_+p_2k_-p_2 \\
& + (\mathcal{F}_1\mathcal{F}_2^\star + \mathcal{F}_1^\star\mathcal{F}_2)(k_+p_1k_-p_2 + k_-p_1k_+p_2)\} \\
& + \frac{e^2|\mathcal{M}|^2}{m_e^2q^4}\{(-m_e^2 + k_+k_-)[p_1^2qp_2^2 + p_2^2qp_1^2 \\
& + q^2p_1p_2^2 - p_1^2p_2^2q^2 - 2p_1p_2qp_1qp_2] \\
& + 2qk_-qk_+(p_1^2p_2^2 - p_1p_2^2) \\
& + 2k_-p_1k_+p_1(p_2^2q^2 - qp_2^2) \\
& + 2k_-p_1k_+p_2(p_1^2q^2 - qp_1^2) \\
& + 2(qp_1qp_2 - q^2p_1p_2)(k_+p_1k_-p_2 + k_+p_2k_-p_1) \\
& + 2(p_1p_2qp_2 - p_2^2qp_1)(k_+p_1k_-q + k_-p_1k_+q) \\
& + 2(p_1p_2qp_1 - p_1^2qp_2)(k_+p_2k_-q + k_-p_2k_+q)\} \\
& + \frac{e^2}{m_e^2q^4}\epsilon^{\mu\nu\rho\sigma}k_{-\mu}p_{1\nu}p_{2\rho}k_{+\sigma} \\
& \times \{(k_+p_1 - k_-p_1)(\mathcal{F}_1^\star\mathcal{M} + \mathcal{F}_1\mathcal{M}^\star) \\
& + (k_+p_2 - k_-p_2)(\mathcal{F}_2^\star\mathcal{M} + \mathcal{F}_2\mathcal{M}^\star)\}.
\end{aligned} \tag{4.2}$$

The structure of (4.2) implies that there is no interference between electric and magnetic form factors in the decay widths of these decays. Additionally, one finds for the decay of the $K_\mathrm{L}$ that there is no interference between electric form factors of lowest and next-to-leading order, too. This feature is due to their different behaviour under exchange of pion momenta. $K_\mathrm{L}$ branching ratios thus consist of three distinct contributions. The more general case of interference between electric form factors of different orders is present in the $K^+$ decay. Phase space integrations are performed numerically with the Fortran event generator RAMBO [32].

### 4.2 Numerical analysis of $K_\mathrm{L} \to \pi^+\pi^-e^+e^-$

In the following, branching ratios (BRs) for different cuts in $q^2$, i.e. for different lower bounds on $(k_+ + k_-)^2$, and the BR over the entire phase space are listed. $q^2$ may vary between $4m_e^2$ and $(m_K - 2m_\pi)^2$. Throughout this analysis, the central values of experimental numbers are used for the branching ratios with certain cuts in $q^2$. The error of a branching ratio is only given if it is calculated over the whole phase space. It should be pointed out (compared to [4]) that the KTeV data, on which I will rely in the following analysis, are corrected for the entire phase space [11,15,16].

**Table 1.** Magnetic and tree-level contributions to the branching ratio of $K_\mathrm{L} \to \pi^+\pi^-e^+e^-$ for different cuts in $q^2$ and for the entire phase space

| $q^2 >$ (MeV$^2$) | Magnetic BR [$10^{-8}$] | Tree-level BR [$10^{-8}$] |
|---|---|---|
| $2^2$ | 18.20 | 9.8 |
| $10^2$ | 9.31 | 2.95 |
| $20^2$ | 5.61 | 1.33 |
| $30^2$ | 3.65 | 0.71 |
| $40^2$ | 2.42 | 0.41 |
| $60^2$ | 1.06 | 0.16 |
| $80^2$ | 0.44 | 0.061 |
| $100^2$ | 0.16 | 0.024 |
| $120^2$ | 0.053 | 0.009 |
| $180^2$ | 0.00025 | 0.0001 |
| entire p.s. | $21.2 \pm 9.0$ | $12.8 \pm 1.0$ |

Using ansatz (3.6) and the experimental numbers of [11] as input for the magnetic contribution to the branching ratio, I find the results collected in Table 1. Neglecting the energy dependent part in (3.6) one reproduces the results in [3]. Obviously, consideration of the energy dependent magnetic form factor in (3.6) increases the results compared to a constant magnetic form factor, particularly for low cuts [3]. Unfortunately, the errors of the parameters entering into the magnetic contribution to the BR are rather large [11]; thus, the magnetic branching ratio over the whole phase space has a considerable uncertainty.

The tree-level form factors of (3.4) give rise to the results collected in column three of Table 1. Comparison with the results in [3] shows that the numbers obtained are rather different, but this is due to different values of $F$ and $G_8$. Here, we use $F = 92.4\,\mathrm{MeV}$ and the canonical $|G_8|$. The error of the BR over the entire phase space in the last line comes from numerics and reflects the $1/q^4$ behaviour of the squared amplitude. Table 1 also shows very clearly the importance of the $q^2$ range between $4m_e^2$ and $4\,\mathrm{MeV}^2$ that was not considered in [4]. The importance of this small $q^2$ range is understood from the plot of the differential decay widths of the individual contributions to the decay in Fig. 6.

The $\mathcal{O}(p^4)$ electric form factors depend via (3.9) on $(N_{14}^\mathrm{r}(\mu) - N_{15}^\mathrm{r}(\mu) - 3(N_{16}^\mathrm{r}(\mu) - N_{17})) =: X(\mu)$, hence electric next-to-leading-order contributions to the branching ratios are given as functions of $X$. The derived branching ratios are listed in Table 2 and allow in principle for an extraction of the whole combination of LECs. $X$ is counted in units of $10^{-2}$. The results collected in Table 2 exhibit

**Table 2.** Contributions of loops and electric counterterms to the branching ratio of $K_{\rm L} \to \pi^+\pi^-e^+e^-$ for different cuts in $q^2$ and for the entire phase space, given as functions of the combination $(N_{14}^{\rm r}(\mu) - N_{15}^{\rm r}(\mu) - 3(N_{16}^{\rm r}(\mu) - N_{17})) =: X(\mu)[10^{-2}]$ of weak LECs. The error is due to the uncertainty of $L_9^{\rm r}$

| $q^2 > (\,\mathrm{MeV}^2)$ | Loops+counterterms BR $[10^{-8}]$ |
|---|---|
| $2^2$ | $0.87 + 0.46X + 0.06X^2$ |
| $10^2$ | $0.86 + 0.45X + 0.06X^2$ |
| $20^2$ | $0.84 + 0.44X + 0.06X^2$ |
| $30^2$ | $0.80 + 0.42X + 0.05X^2$ |
| $40^2$ | $0.75 + 0.39X + 0.05X^2$ |
| $60^2$ | $0.61 + 0.32X + 0.04X^2$ |
| $80^2$ | $0.46 + 0.23X + 0.03X^2$ |
| $100^2$ | $0.30 + 0.16X + 0.02X^2$ |
| $120^2$ | $0.18 + 0.09X + 0.01X^2$ |
| $180^2$ | $0.007 + 0.003X + 0.0004X^2$ |
| entire p.s. | $0.87 \pm 0.19 + (0.46 \pm 0.03)X + 0.06X^2$ |

**Table 3.** Contributions of loops and electric counterterms to the branching ratio of $K_{\rm L} \to \pi^+\pi^-e^+e^-$ for different cuts in $q^2$ and for the entire phase space, given as functions of the combination $(N_{16}^{\rm r} - N_{17}) =: x\ [10^{-2}]$ of weak LECs. $(N_{14}^{\rm r}(m_\rho) - N_{15}^{\rm r}(m_\rho)) = -0.019$ was used

| $q^2 > (\mathrm{MeV}^2)$ | Loops+counterterms BR $[10^{-8}]$ |
|---|---|
| $2^2$ | $0.22 - 0.68x + 0.54x^2$ |
| $10^2$ | $0.22 - 0.67x + 0.53x^2$ |
| $20^2$ | $0.21 - 0.66x + 0.52x^2$ |
| $30^2$ | $0.20 - 0.63x + 0.49x^2$ |
| $40^2$ | $0.19 - 0.59x + 0.46x^2$ |
| $60^2$ | $0.16 - 0.48x + 0.37x^2$ |
| $80^2$ | $0.12 - 0.36x + 0.27x^2$ |
| $100^2$ | $0.08 - 0.24x + 0.18x^2$ |
| $120^2$ | $0.05 - 0.14x + 0.10x^2$ |
| $180^2$ | $0.002 - 0.005x + 0.004x^2$ |
| entire p.s. | $0.22 \pm 0.11 - (0.68 \pm 0.16)x + 0.54x^2$ |

very clearly the entire contribution of the involved weak local counterterms to the electric order $p^4$ branching ratios.

With the help of (3.10), we extract for the combination $(N_{14}^{\rm r}(m_\rho) - N_{15}^{\rm r}(m_\rho))$ a central value of $-0.019$; therefore, the next-to-leading-order electric form factors effectively depend only on $(N_{16}^{\rm r}(\mu) - N_{17}) =: x(\mu)$ and electric contributions of order $p^4$ to the branching ratios can also be expressed as functions of $x$, again counted in units of $10^{-2}$. The derived branching ratios are listed in Table 3. The error in Table 3 was estimated by taking into account the uncertainties of $L_9^{\rm r}$ and $(N_{14}^{\rm r} - N_{15}^{\rm r})$.

The numbers in Tables 2 and 3 cannot be compared immediately to the results in [3], since the corresponding branching ratios were expressed as functions of a different combination of LECs, $w_{\rm L}$ [3]. It turns out that $w_{\rm L}$ is related to the used $N_i$ through $w_{\rm L} = 8\pi^2[-N_{14} + N_{15} + N_{16} - N_{17}]$.

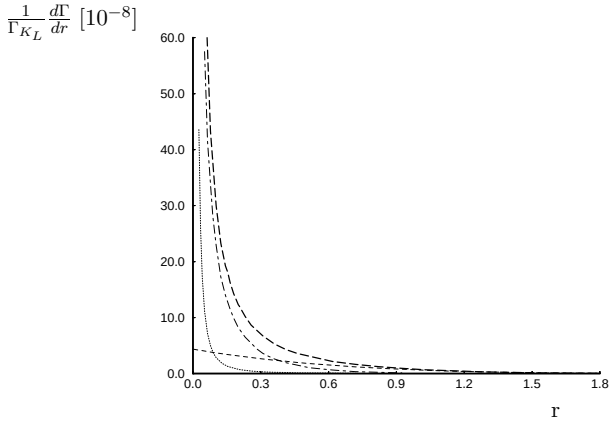


**Fig. 6.** Differential decay width $\frac{1}{\Gamma_{K_{\rm L}}}\frac{d\Gamma}{dr}$ for $(N_{16}^{\rm r}(m_\rho) - N_{17}) = -0.014$; $r := q^2/m_\pi^2$. The dotted line is the tree-level contribution, the dashed line refers to loops and counterterms, the dot-dashed line refers to the magnetic part. The thick long-dashed line is the sum. $\Gamma_{K_{\rm L}}$ is the total width of the $K_{\rm L}$. For cuts with $q^2 > (130\,\mathrm{MeV})^2$ the differential decay width is dominated by the contributions of the electric $\mathcal{O}(p^4)$ amplitude, i.e. loops and electric counterterms

It is obvious from Tables 2 and 3 that the electric $\mathcal{O}(p^4)$ contributions are nearly insensitive to changes of the cut below $\sim (40\,\mathrm{MeV})^2$. This feature becomes also clear from inspection of Fig. 6.

Theory finally predicts as central value of $\mathrm{BR}(K_{\rm L} \to \pi^+\pi^-e^+e^-)$ over the entire phase space $[21.2 + 12.8 + 0.87 + 0.46X + 0.06X^2] \cdot 10^{-8}$, with $X = (N_{14}^{\rm r} - N_{15}^{\rm r} - 3(N_{16}^{\rm r} - N_{17}))[10^{-2}]$. Comparison with the branching ratio obtained in [1], $\mathrm{BR} = [18\ (\mathrm{magn.}) + 13\ (\mathrm{tree}) + 0.4\ (\mathrm{CR})] \cdot 10^{-8}$, shows that inclusion of the magnetic form factor of [11] increases the magnetic BR considerably. Also the total $\mathcal{O}(p^4)$ electric contribution of Table 2 changes the result to some extent.

In the following, the obtained theoretical BR over the entire phase space from Table 3 will be compared to the most recent available data to extract values for $(N_{16}^{\rm r}(m_\rho) - N_{17})$. It should be mentioned that possible values of the related combination $w_{\rm L}$ of LECs were estimated in [4] by comparing with the then recent BR. However, a theoretical cut of $q^2 = (2\,\mathrm{MeV})^2$ was applied and the energy dependence of the magnetic form factor (3.6) was not taken into account.

I focus on the data of the KTeV collaboration, but for completeness one should mention that a Japanese group obtained a BR of $[4.4 \pm 1.3(\mathrm{stat.}) \pm 0.5(\mathrm{syst.})] \cdot 10^{-7}$ [6], based on 13 events, and that the NA48 experiment at CERN recently reported a preliminary BR of $(3.1 \pm 0.3) \cdot 10^{-7}$ [7,8]. In the last years, the KTeV result for the branching ratio was subject to numerous analyses and the errors improved quite a lot. The first published BR was based on a sample of 46 events and it was found to be $[3.2 \pm 0.6(\mathrm{stat.}) \pm 0.4(\mathrm{syst.})] \cdot 10^{-7}$ [5]. A new analysis based on the full 1997 data set reported a BR of $[3.32 \pm$

**Table 4.** Comparison of model predictions (WDM, FM) and the two possible values extracted from data for the combination $(N_{14}^{\rm r} - N_{15}^{\rm r}) - (N_{16}^{\rm r} - N_{17})$ at $m_\rho$

| Model | Pred. | $(N_{14}^{\rm r} - N_{15}^{\rm r}) - x_1$ | $(N_{14}^{\rm r} - N_{15}^{\rm r}) - x_2$ |
|---|---|---|---|
| WDM | $-0.004$ | | |
| FM | $-0.007 k_f$ | $-0.046 \pm 0.036$ | $-0.005 \pm 0.036$ |

$0.14(\text{stat.}) \pm 0.28(\text{syst.})] \cdot 10^{-7}$ with a much better statistical error [12]. I am going to use the latest available (preliminary) numbers which were again obtained from the 1997 data set by considering the parameterization in (3.6) [15,16]: $\text{BR} = [3.63 \pm 0.11(\text{stat.}) \pm 0.14(\text{syst.})] \cdot 10^{-7}$.

It is clear that it is not possible to determine unambiguously the value of $x$ only by comparison with the experiment. The two possible values of $x$ are

$$\begin{aligned} (N_{16}^{\rm r}(m_\rho) - N_{17})_1 = \ x_1 \ &= (2.7 \pm 3.6) \cdot 10^{-2}, \\ (N_{16}^{\rm r}(m_\rho) - N_{17})_2 = \ x_2 \ &= (-1.4 \pm 3.6) \cdot 10^{-2}. \end{aligned} \quad (4.3)$$

The large error is mostly ($\sim 80\%$) due to the uncertainty of the magnetic BR. There is even a small overlap of the two ranges of $x_1$ and $x_2$. Moreover, it should be stressed that comparison with the BR over the entire phase space is not the best possibility to extract values for the LECs, since the BR over the whole phase space is dominated by the tree level and the magnetic amplitude. In addition, Fig. 6 suggests that one could extract a value to a better precision for much higher cuts in $q^2$, but this is not possible at the moment. On the other hand, such an extraction would suffer from smaller statistics. Nevertheless, the central values in (4.3) are very different and one can appeal to models of weak counterterm couplings to distinguish between the two solutions. The weak deformation model (WDM) and the factorization model (FM) [22] make predictions about the involved LECs, but apart from a free parameter of the FM, $N_{14}^{\rm r}$ and $N_{16}^{\rm r}$ depend in both models on the contact term coupling $H_1$ from the strong counterterm Lagrangian [19]. Therefore, it is necessary to compare $(N_{14}^{\rm r} - N_{15}^{\rm r}) - (N_{16}^{\rm r} - N_{17})$ to the experimental values, since in this combination $H_1$ drops out. The comparison of prediction and experiment is given in Table 4. $k_f$ parameterizes the factorization hypothesis and is expected to be of $\mathcal{O}(1)$. Comparison with the results in Table 4 gives $k_{f1} \simeq 6.4 \pm 5.0$ and $k_{f2} \simeq 0.7 \pm 5.0$, respectively. First of all, it is remarkable to find the central value of $x_2$ to be in such good agreement with the predictions of the two models. Secondly, the errors are big enough to dampen too much enthusiasm, but in any case the solution $(N_{16}^{\rm r}(m_\rho) - N_{17}) = -0.014$ is clearly favoured by both models. Moreover, both models and also the results of [33] suggest that $N_{17}$ vanishes individually, so one can even go one step further and assume that

$$N_{16}^{\rm r}(m_\rho) = (-1.4 \pm 3.6) \cdot 10^{-2}\ , \quad N_{17} = 0. \quad (4.4)$$

Additional support comes from the null measurement of interference between electric direct emission and bremsstrahlung in the $K^+ \to \pi^+\pi^0\gamma$ amplitude in [17], since this indicates that the combination $(N_{14}^{\rm r} - N_{15}^{\rm r} - N_{16}^{\rm r} - N_{17}) \simeq 0$ or very small [23,25]. Assumption (4.4), however, is only true for a certain class of models and one should take into account other approaches, too, e.g. the modified FM (FMV) approach [34,35] which was originally introduced to estimate $\mathcal{O}(p^6)$ corrections to radiative kaon decays. This model can also be used to parameterize LECs and it predicts in general a $N_{17}$ different from zero. In any case, solution $x_2$ is also supported by the results in [35]. We will consider the FMV more closely in the next section.

If one's trust in the models used above were big enough, one could even use (4.4) to calculate the contact term coupling $H_1$ of [19] and, as a consequence, calculate $N_{14}^{\rm r}$ and $N_{15}^{\rm r}$, but this does not seem to make much sense. In any case, assumption (4.4) serves as a solid starting point for the analysis of the $K^+$ decay.

**Table 5.** Magnetic and tree-level contributions to the branching ratio of $K^+ \to \pi^+\pi^0 e^+ e^-$ for different cuts in $q^2$ and for the entire phase space. The error of the magnetic part is due to experimental uncertainties of $|A_4|$, whereas the error of the tree-level result comes from numerics; additionally, there is an intrinsic uncertainty because of the $G_{27}$ coupling

| $q^2 > (\text{MeV}^2)$ | Magnetic BR $[10^{-8}]$ | Tree-level BR $[10^{-8}]$ |
|---|---|---|
| $2^2$ | 5.33 | 254.20 |
| $10^2$ | 2.84 | 74.33 |
| $20^2$ | 1.80 | 32.51 |
| $30^2$ | 1.23 | 17.35 |
| $40^2$ | 0.86 | 10.04 |
| $60^2$ | 0.42 | 3.75 |
| $80^2$ | 0.19 | 1.46 |
| $100^2$ | 0.083 | 0.56 |
| $120^2$ | 0.031 | 0.20 |
| $180^2$ | 0.0002 | 0.002 |
| entire p.s. | $6.14 \pm 1.3$ | $330 \pm 15$ |

### 4.3 Numerical analysis of $K^+ \to \pi^+\pi^0 e^+ e^-$

As in the previous case, there is no interference between magnetic and electric parts of the amplitude. Because of the absence of a symmetry relation between the electric form factors as in the $K_{\rm L}$ decay, however, this time there is interference between the tree-level amplitude and loops and electric counterterms.

For the purely magnetic part of the branching ratio, the value of (3.17) is used. The results are collected in the second column of Table 5. As in Sect. 4.2, I only quote the error associated with $|A_4|$ for the branching ratio over the entire phase space.

In the following, I present the individual BRs due to electric form factors of lowest and next-to-leading order as well as the total electric branching ratios, which allows for an extraction of the interference contribution. The BR due to the lowest order is generated by the tree-level form factors given in (3.15). They produce a branching ratio that

**Table 6.** Electric $\mathcal{O}(p^4)$ contribution to the branching ratio of $K^+ \to \pi^+\pi^0 e^+e^-$ for cuts in $q^2$ and for the entire phase space considering the error of (4.4). $(N_{14}^{\rm r} + 2N_{15}^{\rm r}) := z$ $[10^{-2}]$

| $q^2 > (\mathrm{MeV}^2)$ | Loops+counterterms BR $[10^{-9}]$ |
|---|---|
| $2^2$ | $46 + 0.51z + 0.042z^2$ |
| $10^2$ | $2.52 + 0.48z + 0.042z^2$ |
| $20^2$ | $1.68 + 0.46z + 0.041z^2$ |
| $30^2$ | $1.43 + 0.43z + 0.039z^2$ |
| $40^2$ | $1.25 + 0.40z + 0.036z^2$ |
| $60^2$ | $0.94 + 0.32z + 0.030z^2$ |
| $80^2$ | $0.67 + 0.24z + 0.022z^2$ |
| $100^2$ | $0.43 + 0.16z + 0.015z^2$ |
| $120^2$ | $0.25 + 0.09z + 0.009z^2$ |
| $180^2$ | $0.01 + 0.004z + 0.0004z^2$ |
| entire p.s. | $122 \pm 134 + (0.56 \pm 0.27)z + 0.043z^2$ |

**Table 7.** Contributions of the total electric part of the amplitude, $\mathcal{O}(p^2)$ and $\mathcal{O}(p^4)$, to the branching ratio of $K^+ \to \pi^+\pi^0 e^+e^-$ for cuts in $q^2$ and for the entire phase space with consideration of the error of (4.4). $(N_{14}^{\rm r} + 2N_{15}^{\rm r}) := z$ $[10^{-2}]$

| $q^2 > (\mathrm{MeV}^2)$ | Electric $\mathcal{O}(p^2) + \mathcal{O}(p^4)$ BR $[10^{-9}]$ |
|---|---|
| $2^2$ | $2745 + 2.69z + 0.042z^2$ |
| $10^2$ | $785.6 + 2.57z + 0.042z^2$ |
| $20^2$ | $354.3 + 2.29z + 0.041z^2$ |
| $30^2$ | $193.8 + 2.09z + 0.039z^2$ |
| $40^2$ | $115.6 + 1.83z + 0.036z^2$ |
| $60^2$ | $46.3 + 1.32z + 0.030z^2$ |
| $80^2$ | $19.8 + 0.88z + 0.022z^2$ |
| $100^2$ | $8.40 + 0.52z + 0.015z^2$ |
| $120^2$ | $3.34 + 0.27z + 0.009z^2$ |
| $180^2$ | $0.06 + 0.008z + 0.0004z^2$ |
| entire p.s. | $3783 \pm 350 + (2.74 \pm 0.82)z + 0.043z^2$ |

is much larger than that of $K_{\rm L} \to \pi^+\pi^- e^+e^-$; it is given in the third column of Table 5. As already mentioned, the tree-level value of $G_{27}$ is used for the numerical analysis and this clearly introduces an intrinsic uncertainty in the predictions. The error associated with the choice of $G_8$ is very small for the tree level. For loops and counterterm contributions we choose again the canonical $|G_8|$. For completeness, I quote the error arising from numerics because of the $1/q^4$ behaviour of the tree-level amplitude.

The $\mathcal{O}(p^4)$ form factors contain the combinations of LECs given in (3.19). Here, I use the assumption of (4.4) and thus express the derived branching ratios as functions of $(N_{14}^{\rm r}(\mu) + 2N_{15}^{\rm r}(\mu)) =: z(\mu)$ (in units of $10^{-2}$). The results are given in Table 6. The total electric contributions form the tree level, loops and counterterms are collected in Table 7. From this analysis it is clear that it will be very difficult to isolate the electric $\mathcal{O}(p^4)$ corrections to branching ratios with small or no cuts in $q^2$. Again, the importance of the last step from a cut of $4\,\mathrm{MeV}^2$ to no cut at all should be mentioned. Comparison with the previous $K_{\rm L}$ decay shows that the tree-level contribution, although it is suppressed by isospin symmetry, dominates the BR and that it is much more important than for the $K_{\rm L}$ decay, where the tree level was $\epsilon$-suppressed.

Finally, using only the central values of input quantities and applying assumption (4.4), $N_{16}^{\rm r}(m_\rho) = -0.014$ and $N_{17} = 0$, the central value of the branching ratio for $K^+ \to \pi^+\pi^0 e^+e^-$ over the entire phase space is predicted to be $[6 \; + \; 378 + 0.27z + 0.004z^2] \cdot 10^{-8}$.

### 4.4 Dependence on counterterm models

In Sect. 4.2 it was claimed that also the modified factorization model (FMV) of [34,35] favours $(N_{16}^{\rm r}(m_\rho) - N_{17}) = -0.014$. We will now clarify why this is so. In [34,35], the authors introduced a different approach compared to the one used in [22] to incorporate interactions between pseudoscalars and vector and axial-vector resonances. Factorization, however, was still an important ingredient. Originally used to estimate order $p^6$ corrections to kaon decays, their framework was also extended to parameterize combinations of weak LECs in terms of two positive $\mathcal{O}(1)$ parameters, $\eta_V$ and $\eta_A$. According to [35], however, one finds that the weak LECs we are interested in, $N_{14}^{\rm r}$, $N_{15}^{\rm r}$, $N_{16}^{\rm r}$ and $N_{17}$, do not depend on the factorization hypothesis. Hence, one should consider the parameterizations of combinations of these LECs in terms of $\eta_V$ and $\eta_A$ as model independent. Of course, these parameterizations of combinations of LECs still depend on the formalism applied to incorporate vector and axial-vector resonances [35][1].

In the FMV, the relations $(N_{14}^{\rm r} - N_{15}^{\rm r}) = -0.020\eta_V + 0.004\eta_A$ and $(N_{14}^{\rm r} - N_{15}^{\rm r}) - 3(N_{16}^{\rm r} - N_{17}) = -0.004\eta_V + 0.018\eta_A$ hold. Comparison with the two possible values of $(N_{16}^{\rm r} - N_{17})$ in (4.3) gives the following results for the two parameters: for $(N_{16}^{\rm r}(m_\rho) - N_{17}) = 0.027$, one finds

$$\eta_{V_1} = -0.2 \pm 1.1 \quad \text{and} \quad \eta_{A_1} = -5.6 \pm 5.8. \tag{4.5}$$

Using $(N_{16}^{\rm r}(m_\rho) - N_{17}) = -0.014$, one calculates for the FMV parameters

$$\eta_{V_2} = 1.3 \pm 1.1 \quad \text{and} \quad \eta_{A_2} = 1.6 \pm 5.8. \tag{4.6}$$

Of course, the errors are very large, but even then the second pair of values in (4.6) fits much better than the values of (4.5). Using the parameterization $(N_{14}^{\rm r} - N_{15}^{\rm r}) - 3(N_{16}^{\rm r} + N_{17}) = 0.05\eta_V - 0.04\eta_A$, one determines $N_{17} = -0.009\eta_V + 0.0097\eta_A = 0.4 \cdot 10^{-2}$. Thus, we rather find for $N_{16}^{\rm r}$ and $N_{17}$ with the values of (4.6)

$$N_{16}^{\rm r}(m_\rho) = (-1.0 \pm 4.6) \cdot 10^{-2}, \qquad N_{17} = (0.4 \pm 4.6) \cdot 10^{-2} \tag{4.7}$$

In fact, this result is not too different from the hypothesis in (4.4).

Despite the big uncertainties of the values of the parameters $\eta_V$ and $\eta_A$, one nevertheless can use the central

[1] I thank J. Portolés for useful comments on this topic

**Table 8.** Total electric branching ratio of $K^+ \to \pi^+\pi^0 e^+e^-$ for cuts in $q^2$ and for the entire phase space relying on the values of the LECs calculated in (4.7) and (4.8). No errors are taken into account

| $q^2 > (\mathrm{MeV}^2)$ | Electric $\mathcal{O}(p^2)+\mathcal{O}(p^4)$ BR $[10^{-9}]$ |
|---|---|
| $2^2$ | 2923 |
| $10^2$ | 873 |
| $20^2$ | 431 |
| $30^2$ | 253 |
| $40^2$ | 164 |
| $60^2$ | 78 |
| $80^2$ | 39 |
| $100^2$ | 20 |
| $120^2$ | 9 |
| $180^2$ | 0.24 |
| entire p.s. | 3683 |

values to calculate other LECs, especially $N_{14}^{\mathrm{r}}$ and $N_{15}^{\mathrm{r}}$. Probably this is equally daring as the option of calculating $H_1$, but if one truly "believed" in the FMV with the results of (4.6), one could make a parameter-free prediction for the electric part of the branching ratio. According to [35], we have $2N_{14}^{\mathrm{r}} + N_{15}^{\mathrm{r}} = 0.08\eta_V$. Using the experimental result $(N_{14}^{\mathrm{r}} - N_{15}^{\mathrm{r}}) = -0.019$, one calculates

$$N_{14}^{\mathrm{r}}(m_\rho) = 2.8 \cdot 10^{-2},$$
$$N_{15}^{\mathrm{r}}(m_\rho) = 4.7 \cdot 10^{-2}. \qquad (4.8)$$

The results for the electric branching ratios obtained with these values for the counterterm couplings are listed in Table 8. According to Tables 6 and 7, one finds that $\mathcal{O}(p^4)$ corrections become more important for higher cuts in $q^2$ and that branching ratios for lower cuts are dominated by the tree level. E.g. for a cut of $(10\,\mathrm{MeV})^2$, the tree-level BR is modified by $\mathcal{O}(p^4)$ corrections and by the interference between the two electric contributions by about 17%, whereas for a cut of $(80\,\mathrm{MeV})^2$ the result is increased by roughly 160%. It is clear that the interference also gives rise to an important part of the enhancement of the BR. Finally, one should note that the estimated couplings in (4.7) and (4.8) are in a range where one could expect them but it is also true that the uncertainties involved are too big to make a more precise statement about the couplings and the $K^+$ decay width.

## 5 Conclusions

I considered the non-leptonic decays $K_{\mathrm{L}} \to \pi^+\pi^- e^+e^-$ and $K^+ \to \pi^+\pi^0 e^+e^-$ within the framework of chiral perturbation theory. First of all, the amplitudes of the decays have been given up to order $p^4$ in a very explicit way and a consistency check on parts of the weak counterterm Lagrangian of CHPT was performed: all divergences are properly removed.

The main reason to focus on $K_{\mathrm{L}} \to \pi^+\pi^- e^+e^-$ in this paper is provided by the possibility of extracting the combination $(N_{16}^{\mathrm{r}}(\mu) - N_{17})$ of weak LECs from experimental results. The latest value of the preliminary branching ratio, $\mathrm{BR}(K_{\mathrm{L}} \to \pi^+\pi^- e^+e^-) = (3.63 \pm 0.11 \pm 0.14) \cdot 10^{-7}$ [15,16], and the values of the parameters of the magnetic form factor [11], both obtained by the KTeV collaboration, were used for the numerical analysis of the decay.

The introduction of an energy dependent magnetic form factor yields an important correction to the older calculations in [1–3], since it increases the magnetic contribution to the branching ratio considerably. The (preliminary) value for the branching ratio and the parameters of the magnetic form factor were obtained from the analysis of the data set of 1997 which contains more than 1800 events [11]. Comparison with earlier experimental results shows that the errors of the measured quantities became quite smaller due to the better statistics, but the uncertainties are still too big to make precise predictions.

Comparison with experiment yields two possible values of the LEC combination $(N_{16}^{\mathrm{r}}(m_\rho) - N_{17})$; thus, one has to consult theoretical approaches about weak counterterm couplings to distinguish between the possible solutions. All models that have been considered (weak deformation model WDM [22], factorization model FM [22], modified factorization model FMV [34,35]) prefer the same value of $(-1.4 \pm 3.6) \cdot 10^{-2}$. Of course, the error, which is mainly due to the experimental uncertainties of the two parameters of the magnetic amplitude, is quite large, but nevertheless the obtained result is reasonable compared to $(N_{14}^{\mathrm{r}}(m_\rho) - N_{15}^{\mathrm{r}}(m_\rho)) = -1.9 \cdot 10^{-2}$ and it rests upon a firm theoretical ground.

On the other hand, the central value of $(N_{16}^{\mathrm{r}} - N_{17})$ is almost in perfect agreement with the FM and WDM predictions. One also derives central values for the two parameters of the FMV that are in good agreement with the expectations.

Since 1997, much more data have been collected by the KTeV group and therefore one can hope that a new analysis of the much larger set of events can reduce the experimental uncertainties. As already pointed out in Sect. 4.2, it should also be possible to extract the value of $(N_{16}^{\mathrm{r}} - N_{17})$ to a better precision by comparing the theoretical results with branching ratios for higher cuts in $q^2$ (e.g. $\sim (40\,\mathrm{MeV})^2$), since the contributions from loops and counterterms become much more important for higher cuts than for the entire phase space.

To be able to make a useful prediction for the $K^+$ decay, one has to rely on additional theoretical assumptions. First, I followed the predictions of the FM and WDM and assumed that the extracted value $-1.4 \cdot 10^{-2}$ is produced solely by $N_{16}^{\mathrm{r}}$, and that $N_{17} = 0$. It is therefore possible to express the branching ratio for $K^+ \to \pi^+\pi^0 e^+e^-$ as a function of $(N_{14}^{\mathrm{r}} + 2N_{15}^{\mathrm{r}})$.

Contrary to the decay of the $K_{\mathrm{L}}$, there exists an interference between the tree-level amplitude and the electric $\mathcal{O}(p^4)$ amplitude. In general, it is found that the branching ratio due to the electric part of the decay amplitude clearly dominates over the magnetic contributions. More-

over, it is the tree level that produces by far the most important contributions to the BR over the entire phase space as well as for a wide range of cuts in $q^2$.

An extraction of the combination $(N_{14}^{\rm r} + 2N_{15}^{\rm r})$ from the branching ratio over the entire phase space is almost impossible, but according to the discussion in Sect. 4.4, with a scan of the $q^2$ spectrum it is more likely to extract values for $(N_{14}^{\rm r} + 2N_{15}^{\rm r})$, especially for cuts larger than $\sim (60\,\mathrm{MeV})^2$. Obviously the experimental error of the magnetic part of the amplitude and the error of the combination $(N_{16}^{\rm r} - N_{17})$ will not make it easier to extract a reasonable value, but hopefully new results from KTeV (and from CERN) also help to improve the predictive power of this analysis.

Whereas the analysis summarized so far was based on conservative assumptions, I also speculated about extracting values for $N_{14}^{\rm r}$, $N_{15}^{\rm r}$, $N_{16}^{\rm r}$ and $N_{17}$. Referring to the FMV, the two parameters of the model were estimated using the available data and the extracted value of $(N_{16}^{\rm r} - N_{17})$. The central values of these parameters were further used to estimate the central values of the four low-energy couplings $N_{14}^{\rm r}$, $N_{15}^{\rm r}$, $N_{16}^{\rm r}$ and $N_{17}$ and to make a "prediction" of the $K^+$ branching ratio without any free parameter. Although the errors are big, the obtained values for the LECs seem to be reasonable.

*Acknowledgements.* Most of this work was done in Vienna and I would like to thank G. Ecker for his help during a long time. I thank G. Isidori, G. D'Ambrosio, J. Portolés and R. Escribano for helpful discussions on physics and computing. I am grateful for important comments on the experimental input by T. Barker, B. Cox and S. Ledovskoy from the KTeV collaboration. Finally, G. Pancheri should be mentioned since she made it possible for me to come to the LNF in Frascati.

## Appendix

## A Loop functions

All loop integrals in this work can be reduced to a basis of three scalar integrals:

$$\begin{aligned}
\mathrm{i}A(m^2) &= \int \frac{\mathrm{d}^d k}{(2\pi)^d}\frac{1}{D_1},\\
\mathrm{i}B(q^2,m^2,M^2) &= \int \frac{\mathrm{d}^d k}{(2\pi)^d}\frac{1}{D_2},\\
\mathrm{i}C(q^2,p^2,m^2,M^2) &= \int \frac{\mathrm{d}^d k}{(2\pi)^d}\frac{1}{D_3},
\end{aligned} \tag{A.1}$$

where I introduced the abbreviations $D_1 = [k^2 - m^2]$, $D_2 = [k^2 - m^2][(k-q)^2 - M^2]$ and $D_3 = [k^2 - m^2]$ $[(k-q)^2 - M^2][(k-p)^2 - M^2]$. Indexed loop functions are defined through the following relations:

$$\begin{aligned}
\int \frac{\mathrm{d}^d k}{(2\pi)^d}\frac{k_\mu}{D_2} &= \mathrm{i}q_\mu B_1(q^2,m^2,M^2),\\
\int \frac{\mathrm{d}^d k}{(2\pi)^d}\frac{k_\mu}{D_3} &= \mathrm{i}q_\mu C_1(q^2,p^2,qp,m^2,M^2)\\
&\quad + \mathrm{i}p_\mu C_2(q^2,p^2,qp,m^2,M^2),\\
\int \frac{\mathrm{d}^d k}{(2\pi)^d}\frac{k_\mu k_\nu}{D_2} &= \mathrm{i}g_{\mu\nu} B_{00}(q^2,m^2,M^2)\\
&\quad + \mathrm{i}q_\mu q_\nu B_{11}(q^2,m^2,M^2),\\
\int \frac{\mathrm{d}^d k}{(2\pi)^d}\frac{k_\mu k_\nu}{D_3} &= \mathrm{i}g_{\mu\nu} C_{00}(q^2,p^2,qp,m^2,M^2)\\
&\quad + \mathrm{i}q_\mu q_\nu C_{11}(q^2,p^2,qp,m^2,M^2)\\
&\quad + \mathrm{i}(q_\mu p_\nu + q_\nu p_\mu) C_{12}(q^2,p^2,qp,m^2,M^2)\\
&\quad + \mathrm{i}p_\mu p_\nu C_{22}(q^2,p^2,qp,m^2,M^2).
\end{aligned} \tag{A.2}$$

They can be given explicitly in terms of (A.1). Divergences arise through the scalar loop functions $A$ and $B$ in (A.1). The divergent parts of these functions are isolated in expressions similar to (2.9).

$$\begin{aligned}
&A(m^2)|_{\rm div} = -2m^2\Lambda(\mu),\\
&B(q^2,m^2,M^2)|_{\rm div} = -2\Lambda(\mu),\\
&\Lambda(\mu) = \frac{\mu^{d-4}}{16\pi^2}\left[\frac{1}{d-4} - \frac{1}{2}(\ln(4\pi) + 1 - \gamma_{\rm E})\right].
\end{aligned} \tag{A.3}$$

Apart from $C_{00}$, all $C$-like functions are finite.

## B $K_{\rm L} \to \pi^+\pi^-\gamma^\star$ form factor $\mathcal{F}_{16}^{\rm Ll}$

The electric form factor $\mathcal{F}_1^{\rm L}$ gets contributions from topologies 2 and 3 collected in $\mathcal{F}_{16}^{\rm Ll}$; the first part of $\mathcal{F}_{16}^{\rm Ll}$ is due to the loop particles $(K_1^0, \pi^\pm)$, the second part arises from $(\eta_8, K^\pm)$, and the very last line comes from $(\pi^0, K^\pm)$.

$$\begin{aligned}
\mathcal{F}_{16}^{\rm Ll} = \frac{-\mathrm{i}eG_8}{F}\,\{&-2A(m_\pi^2)\\
&-\frac{1}{2}(q^2+2qp_1)B(q^2,m_\pi^2,m_\pi^2)\\
&+\frac{1}{2(q^2+2qp_1)}\\
&\times[2m_\pi^2(q^2+2qp_1-m_K^2)+m_K^2(m_K^2-q^2-2qp_1)]\\
&\times(B(m_\pi^2,m_K^2,m_\pi^2)-B((p_1+q)^2,m_K^2,m_\pi^2))\\
&+\frac{1}{q^2+2qp_1}[m_K^2(m_\pi^2+p_1p_2+qp_2-q^2-2qp_1)\\
&-2m_\pi^2(p_1p_2+qp_2)]B_1(m_\pi^2,m_K^2,m_\pi^2)\\
&+\frac{1}{2(q^2+2qp_1)}[m_K^2(-2m_\pi^2-q^2-2qp_1-2p_1p_2\\
&-2qp_2)+m_\pi^2(2q^2+4qp_1+4p_1p_2+4qp_2)+2q^4\\
&+q^2(8qp_1+2p_1p_2+2qp_2)+8qp_1^2+4p_1p_2qp_1\\
&+4qp_2qp_1]B_1((p_1+q)^2,m_K^2,m_\pi^2)\\
&+4B_{00}(q^2,m_\pi^2,m_\pi^2)\\
&+\frac{2(p_1p_2+qp_2)}{q^2+2qp_1}\\
&\times[B_{00}(m_\pi^2,m_K^2,m_\pi^2)-B_{00}((p_1+q)^2,m_K^2,m_\pi^2)\\
&+m_\pi^2B_{11}(m_\pi^2,m_K^2,m_\pi^2)\\
&-(m_\pi^2+q^2+2qp_1)B_{11}((p_1+q)^2,m_K^2,m_\pi^2)]
\end{aligned}$$

$$
\begin{aligned}
&- \frac{1}{2}[m_K^2(m_K^2 - q^2 - 2qp_1 - 2m_\pi^2) \\
&+ 2m_\pi^2(q^2 + 2qp_1)]C(m_\pi^2,(p_1+q)^2,m_K^2,m_\pi^2) \\
&+ \frac{1}{2}[m_K^2(-4p_1p_2 - 4m_\pi^2 + m_K^2 - 2q^2 - 4qp_1) \\
&+ m_\pi^2(4p_1p_2 + 4q^2 + 8qp_1)] \\
&\times C_1(m_\pi^2,(p_1+q)^2,m_K^2,m_\pi^2) \\
&+ \frac{1}{2}[m_K^2(-4m_\pi^2 - 6qp_1 - 4p_1p_2 \\
&- 4qp_2 + m_K^2 - 2q^2) \\
&+ 4m_\pi^2(q^2 + 2qp_1 + p_1p_2 + qp_2) \\
&+ 2qp_1(q^2 + 2qp_1)]C_2(m_\pi^2,(p_1+q)^2,m_K^2,m_\pi^2) \\
&+ m_K^2 C_{00}(m_\pi^2,(p_1+q)^2,m_K^2,m_\pi^2) \\
&- 2(m_\pi^2 - m_K^2)C_{00}(m_\pi^2,(p_2+q)^2,m_K^2,m_\pi^2) \\
&+ (2m_K^2p_1p_2 + m_K^2m_\pi^2 - 2m_\pi^2p_1p_2) \\
&\times C_{11}(m_\pi^2,(p_1+q)^2,m_K^2,m_\pi^2) \\
&+ [m_K^2(qp_1 + 2qp_2 + 2m_\pi^2 + 4p_1p_2) \\
&- 2m_\pi^2(qp_2 + 2p_1p_2)]C_{12}(m_\pi^2,(p_1+q)^2,m_K^2,m_\pi^2) \\
&+ [m_K^2(2p_1p_2 + 2qp_2 + m_\pi^2 + qp_1) \\
&- 2m_\pi^2(p_1p_2 + qp_2)] \\
&\times C_{22}(m_\pi^2,(p_1+q)^2,m_K^2,m_\pi^2) - \frac{11}{6}A(m_K^2) \\
&- \frac{1}{9}[m_\pi^2 + 2m_K^2 + 6(2qp_1 + qp_2 + p_1p_2 + q^2)] \\
&\times B(q^2,m_K^2,m_K^2) \\
&+ \frac{1}{18(q^2+2qp_1)} \\
&\times [m_\eta^2(-6(p_1p_2 + qp_2 + q^2 + 2qp_1) \\
&+ 2m_K^2 - 11m_\pi^2) \\
&+ 3m_\pi^2(m_\pi^2 + 6q^2 + 12qp_1 + 2m_K^2 + 6p_1p_2 + 6qp_2)] \\
&\times (B(m_\pi^2,m_\eta^2,m_K^2) - B((p_1+q)^2,m_\eta^2,m_K^2)) \\
&+ \frac{1}{9(q^2+2qp_1)} \\
&\times [9m_\eta^2(m_\pi^2 + p_1p_2 + qp_2 - q^2 - 2qp_1) \\
&+ m_\pi^2(-11m_\pi^2 - 9q^2 - 18qp_1 - 4m_K^2 \\
&- 39p_1p_2 - 39qp_2) + 6m_K^2(q^2 + 2qp_1)] \\
&\times B_1(m_\pi^2,m_\eta^2,m_K^2) \\
&- \frac{1}{9(q^2+2qp_1)} \\
&\times [3m_\eta^2(2q^2 + 4qp_1 + 3p_1p_2 + 3qp_2 + 3m_\pi^2) \\
&+ m_\pi^2(-11m_\pi^2 - 4m_K^2 - 29q^2 - 58qp_1 \\
&- 39p_1p_2 - 39qp_2) \\
&- 4m_K^2(q^2 + 2qp_1) - 72qp_1^2 - 72q^2qp_1 - 18q^4 \\
&- 30q^2p_1p_2 - 30q^2qp_2 - 60qp_1p_1p_2 - 60qp_1qp_2] \\
&\times B_1((p_1+q)^2,m_\eta^2,m_K^2) + 5B_{00}(q^2,m_K^2,m_K^2) \\
&+ \frac{4}{3(q^2+2qp_1)} \\
&\times [(m_\pi^2 + 3p_1p_2 + 3qp_2)B_{00}(m_\pi^2,m_\eta^2,m_K^2) \\
&- (m_\pi^2 + q^2 + 2qp_1 + 3p_1p_2 \\
&+ 3qp_2)B_{00}((p_1+q)^2,m_\eta^2,m_K^2)] \\
&+ \frac{4}{3(q^2+2qp_1)} \\
&\times [m_\pi^2(m_\pi^2 + 3p_1p_2 + 3qp_2)B_{11}(m_\pi^2,m_\eta^2,m_K^2) \\
&- (m_\pi^2(m_\pi^2 + 2q^2 + 4qp_1 + 3p_1p_2 + 3qp_2) \\
&+ q^2(q^2 + 4qp_1 + 3p_1p_2 + 3qp_2) + 4qp_1^2 \\
&+ 6qp_1(qp_2 + p_1p_2))B_{11}((p_1+q)^2,m_\eta^2,m_K^2)] \\
&- \frac{1}{18}[m_\eta^2(-6(p_1p_2 + q^2 + 2qp_1 + qp_2) \\
&- 11m_\pi^2 + 2m_K^2) \\
&+ 3m_\pi^2(6p_1p_2 + 6qp_2 + 6q^2 + 12qp_1 + m_\pi^2 + 2m_K^2)] \\
&\times C(m_\pi^2,(p_1+q)^2,m_\eta^2,m_K^2) \\
&+ \frac{1}{18}[3m_\eta^2(-14m_\pi^2 - 24p_1p_2 - 18qp_1 - 6qp_2 \\
&- 6q^2 - 2m_K^2 + m_\eta^2) + m_\pi^2(24m_K^2 + 30qp_2 \\
&+ 66qp_1 + 48p_1p_2 + 30q^2 + 11m_\pi^2) \\
&+ m_K^2(36qp_1 + 12qp_2 + 12q^2 + 48p_1p_2 + 4m_K^2)] \\
&\times C_1(m_\pi^2,(p_1+q)^2,m_\eta^2,m_K^2) \\
&+ \frac{1}{18}[3m_\eta^2(m_\eta^2 - 2m_K^2 - 14m_\pi^2 \\
&- 12q^2 - 28qp_1 - 24qp_2 - 24p_1p_2) \\
&+ m_\pi^2(11m_\pi^2 + 24m_K^2 + 36q^2 + 76qp_1 \\
&+ 48qp_2 + 48p_1p_2) \\
&+ 4m_K^2(6q^2 + 14qp_1 + 12qp_2 + 12p_1p_2 + m_K^2) \\
&+ 24qp_1(q^2 + qp_2 + p_1p_2 + 2qp_1)] \\
&\times C_2(m_\pi^2,(p_1+q)^2,m_\eta^2,m_K^2) \\
&+ 2(m_K^2 - m_\pi^2)C_{00}(m_\pi^2,(p_2+q)^2,m_\eta^2,m_K^2) \\
&+ \frac{2}{3}(m_\eta^2 + m_K^2 - m_\pi^2)C_{00}(m_\pi^2,(p_1+q)^2,m_\eta^2,m_K^2) \\
&+ \frac{1}{3}[m_\eta^2(5m_\pi^2 + 3qp_1 + 9p_1p_2) \\
&- m_\pi^2(m_\pi^2 + 2m_K^2 + qp_1 + 3p_1p_2) \\
&- 2m_K^2(qp_1 + 3p_1p_2)]C_{11}(m_\pi^2,(p_1+q)^2,m_\eta^2,m_K^2) \\
&+ \frac{1}{3}[m_\eta^2(10m_\pi^2 + 3q^2 + 11qp_1 + 9qp_2 + 18p_1p_2) \\
&- m_\pi^2(2m_\pi^2 + 4m_K^2 + q^2 + 3qp_1 + 3qp_2 + 6p_1p_2) \\
&- 2m_K^2(q^2 + 3qp_1 + 3qp_2 + 6p_1p_2)] \\
&\times C_{12}(m_\pi^2,(p_1+q)^2,m_\eta^2,m_K^2) \\
&+ \frac{1}{3}[m_\eta^2(5m_\pi^2 + 3q^2 + 8qp_1 + 9qp_2 + 9p_1p_2) \\
&- m_\pi^2(m_\pi^2 + 2m_K^2 + q^2 + 2qp_1 + 3qp_2 + 3p_1p_2) \\
&- 2m_K^2(q^2 + 2qp_1 + 3qp_2 + 3p_1p_2)] \\
&\times C_{22}(m_\pi^2,(p_1+q)^2,m_\eta^2,m_K^2) \\
&+ \frac{(d-2)}{2(d-1)} \\
&\times \left[A(m_K^2) + \frac{(q^2 - 4m_K^2)}{2(d-2)}B(q^2,m_K^2,m_K^2)\right]\Bigg\}. \quad \text{(B.1)}
\end{aligned}
$$

## C $K^+ \to \pi^+\pi^0\gamma^\star$ form factors $\mathcal{F}^{+1}_{15,16}$, $\mathcal{F}^{+1}_{25,26}$

The electric form factors $\mathcal{F}_1^+$ and $\mathcal{F}_2^+$ get contributions from topologies 2 and 3. Contributions with an $\eta_8$ in the loop are collected in the expressions $\mathcal{F}^{+1}_{15,25}$, contributions with a pair of any kaon and pion are collected in $\mathcal{F}^{+1}_{16,26}$, respectively. The contributions with an $\eta_8$ read

$$
\begin{aligned}
\mathcal{F}^{+1}_{15} = {} & \frac{-\mathrm{i}eG_8}{F} \\
& \times \Bigg\{ -\frac{1}{9(q^2+2qp_1)(q^2+2qp_1+2qp_2)} \\
& \times [m_\pi^2(6q^2+12qp_1+22qp_2) \\
& + m_K^2(-3q^2-6qp_1-qp_2) \\
& + 6q^2(q^2+4qp_1+4qp_2+p_1p_2) \\
& + 12qp_1(2qp_1+4qp_2+p_1p_2) \\
& + 24qp_2(qp_2+p_1p_2)]A(m_K^2) \\
& + \frac{1}{18(q^2+2qp_1)(q^2+2qp_1+2qp_2)} \\
& \times [3m_\eta^2(-2m_\pi^2+m_K^2-q^2-2qp_1-2p_1p_2) \\
& + m_\pi^2(26m_\pi^2-15m_K^2+13q^2 \\
& + 26qp_1+12qp_2+38p_1p_2) \\
& + m_K^2(m_K^2-q^2-2qp_1-6qp_2-8p_1p_2) \\
& + 6p_1p_2(q^2+2qp_1+2qp_2+2p_1p_2)]A(m_\eta^2) \\
& + \frac{1}{9}(11m_\pi^2-8m_K^2+6qp_2+6p_1p_2)B(q^2,m_K^2,m_K^2) \\
& + \frac{1}{54(q^2+2qp_1)(q^2+2qp_1+2qp_2)} \\
& \times [m_\pi^2m_K^2(-12m_\pi^2+24m_K^2-58q^2 \\
& - 116qp_1-60p_1p_2) \\
& + m_\pi^2p_1p_2(-12q^2-24qp_1-240m_\pi^2 \\
& - 144p_1p_2-144qp_2) \\
& + m_K^2p_1p_2(30m_K^2-60q^2-120qp_1 \\
& - 72qp_2-72p_1p_2) \\
& + m_\pi^4(-28q^2-56qp_1-144qp_2) \\
& + m_K^4(5q^2+10qp_1+36qp_2) \\
& + m_\pi^2(60q^4+240qp_1^2+240q^2qp_1+120q^2qp_2 \\
& + 240qp_1qp_2) \\
& + m_K^2(-24q^4-96qp_1^2-96q^2qp_1 \\
& - 48q^2qp_2-96qp_1qp_2)+3m_K^6-96m_\pi^6] \\
& \times B(m_\pi^2,m_\eta^2,m_K^2) \\
& + \frac{1}{18(q^2+2qp_1)} \\
& \times [m_\eta^2(-3m_\eta^2+8m_K^2-2m_\pi^2-6qp_2-6p_1p_2) \\
& + m_\pi^2(33m_\pi^2-24m_K^2+18qp_2+18p_1p_2)] \\
& \times B((p_1+q)^2,m_\eta^2,m_K^2) \\
& - \frac{1}{18(q^2+2qp_1+2qp_2)} \\
& \times [9m_\eta^2(-2m_\pi^2-q^2-2qp_1-2qp_2-2p_1p_2) \\
& + m_\pi^2(22m_\pi^2+8m_K^2+27q^2+54qp_1 \\
& + 54qp_2+78p_1p_2) \\
& + 6m_K^2(q^2+2qp_1+2qp_2)]B_1(m_\pi^2,m_\eta^2,m_K^2) \\
& + \frac{1}{(q^2+2qp_1)(q^2+2qp_1+2qp_2)} \\
& \times [m_\pi^2m_K^2(-2m_\pi^2-m_K^2+q^2 \\
& + 2qp_1-4qp_2-2p_1p_2) \\
& + m_\pi^2p_1p_2(20m_\pi^2+6q^2+12qp_1+12qp_2+12p_1p_2) \\
& + m_K^2p_1p_2(-m_K^2+q^2+2qp_1+2qp_2+2p_1p_2) \\
& + 4m^4(q^2+2qp_1+3qp_2+2m_\pi^2) \\
& - m_K^4qp_2]B_1(m_\pi^2,m_K^2,m_\eta^2) \\
& + \frac{1}{9(q^2+2qp_1)}[m_\pi^2(-10m_\pi^2+4m_K^2 \\
& - 5q^2-10qp_1+18qp_2+18p_1p_2) \\
& + 4m_K^2(2q^2+4qp_1-3qp_2-3p_1p_2) \\
& + 6q^2(q^2+4qp_1+qp_2+p_1p_2) \\
& + 12qp_1(2qp_1+qp_2+p_1p_2)] \\
& \times B_1((p_1+q)^2,m_\eta^2,m_K^2) \\
& + 2B_{00}(q^2,m_K^2,m_K^2) \\
& + \frac{4(m_\pi^2+3p_1p_2)}{3(q^2+2qp_1+2qp_2)}B_{00}(m_\pi^2,m_\eta^2,m_K^2) \\
& - \frac{2}{(q^2+2qp_1)(q^2+2qp_1+2qp_2)} \\
& \times [2m_\pi^2(2m_\pi^2-m_K^2+q^2+2qp_1+3qp_2+5p_1p_2) \\
& - 3m_K^2(qp_2+p_1p_2) \\
& + 3p_1p_2(q^2+2qp_1+2qp_2+2p_1p_2)] \\
& \times B_{00}(m_\pi^2,m_K^2,m_\eta^2) \\
& - \frac{2}{3(q^2+2qp_1)} \\
& \times [2m_\pi^2+6qp_2+6p_1p_2+2q^2+4qp_1] \\
& \times B_{00}((p_1+q)^2,m_\eta^2,m_K^2) \\
& + \frac{4m_\pi^2(m_\pi^2+3p_1p_2)}{3(q^2+2qp_1+2qp_2)}B_{11}(m_\pi^2,m_\eta^2,m_K^2) \\
& - \frac{2m_\pi^2}{(q^2+2qp_1)(q^2+2qp_1+2qp_2)} \\
& \times [2m_\pi^2(2m_\pi^2-m_K^2+q^2+2qp_1+3qp_2+5p_1p_2) \\
& - 3m_K^2(qp_2+p_1p_2) \\
& + 3p_1p_2(q^2+2qp_1+2qp_2+2p_1p_2)] \\
& \times B_{11}(m_\pi^2,m_K^2,m_\eta^2) \\
& - \frac{4}{3(q^2+2qp_1)} \\
& \times [m_\pi^2(m_\pi^2+2q^2+4qp_1+3qp_2+3p_1p_2) \\
& + q^2(q^2+4qp_1+3qp_2+3p_1p_2) \\
& + qp_1(4qp_1+6qp_2+6p_1p_2)] \\
& \times B_{11}((p_1+q)^2,m_\eta^2,m_K^2) \\
& + \frac{1}{18}[(m_\eta^2(-3m_\eta^2-2m_\pi^2+8m_K^2-6qp_2-6p_1p_2)
\end{aligned}
$$

$$
\begin{aligned}
&+ m_\pi^2(33m_\pi^2 - 24m_K^2 + 18qp_2 + 18p_1p_2)) \\
&\times C(m_\pi^2,(p_1+q)^2,m_\eta^2,m_K^2) \\
&- (m_\eta^2(-3m_\eta^2 + 6m_\pi^2 + 24m_K^2 \\
&+ 18qp_1 - 18qp_2 + 36p_1p_2) \\
&+ m_\pi^2(49m_\pi^2 - 30m_K^2 - 6qp_1 + 30qp_2 + 12p_1p_2) \\
&+ m_K^2(-16m_K^2 - 12qp_1 + 12qp_2 - 24p_1p_2)) \\
&\times C_1(m_\pi^2,(p_1+q)^2,m_\eta^2,m_K^2) \\
&- (m_\eta^2(-3m_\eta^2 + 6m_\pi^2 + 24m_K^2 \\
&+ 18q^2 + 48qp_1 + 36qp_2 + 36p_1p_2) \\
&+ m_\pi^2(49m_\pi^2 - 30m_K^2 - 6q^2 + 32qp_1 \\
&+ 12qp_2 + 12p_1p_2) \\
&+ m_K^2(-16m_K^2 - 12q^2 - 56qp_1 - 24qp_2 - 24p_1p_2) \\
&+ 24qp_1qp_2 + 24qp_1p_1p_2) \\
&\times C_2(m_\pi^2,(p_1+q)^2,m_\eta^2,m_K^2)] \\
&- \frac{1}{3}[(-5m_\eta^2 + m_\pi^2 + 2m_K^2) \\
&\times C_{00}(m_\pi^2,(p_1+q)^2,m_\eta^2,m_K^2) \\
&+ (m_\eta^2(-5m_\pi^2 - 3qp_1 - 9p_1p_2) \\
&+ m_\pi^2(m_\pi^2 + 2m_K^2 + qp_1 + 3p_1p_2) \\
&+ m_K^2(2qp_1 + 6p_1p_2))C_{11}(m_\pi^2,(p_1+q)^2,m_\eta^2,m_K^2) \\
&+ (m_\eta^2(-5m_\pi^2 - 3q^2 - 8qp_1 - 9qp_2 - 9p_1p_2) \\
&+ m_\pi^2(m_\pi^2 + 2m_K^2 + q^2 + 2qp_1 + 3qp_2 + 3p_1p_2) \\
&+ m_K^2(2q^2 + 4qp_1 + 6qp_2 + 6p_1p_2)) \\
&\times C_{22}(m_\pi^2,(p_1+q)^2,m_\eta^2,m_K^2) \\
&+ (m_\eta^2(-10m_\pi^2 - 3q^2 - 11qp_1 - 9qp_2 - 18p_1p_2) \\
&+ m_\pi^2(2m_\pi^2 + 4m_K^2 + q^2 + 3qp_1 + 3qp_2 + 6p_1p_2) \\
&+ m_K^2(2q^2 + 6qp_1 + 6qp_2 + 12p_1p_2)) \\
&\times C_{12}(m_\pi^2,(p_1+q)^2,m_\eta^2,m_K^2)]\Big\}, \qquad \text{(C.1)}
\end{aligned}
$$

$$
\begin{aligned}
\mathcal{F}_{25}^{+\mathrm{l}} = \frac{-\mathrm{i}eG_8}{F}\Bigg\{ & \frac{1}{18(q^2+2qp_1+2qp_2)} \\
&\times (-3q^2 - 6qp_1 - 6qp_2 + 12p_1p_2 + 5m_K^2 + 10m_\pi^2) \\
&\times A(m_K^2) \\
&+ \frac{1}{18(q^2+2qp_1+2qp_2)} \\
&\times (54p_1p_2 + 62m_\pi^2 - 29m_K^2)A(m_\eta^2) \\
&- \frac{1}{54(q^2+2qp_1+2qp_2)} \\
&\times [m_\pi^2(-30q^2 - 60qp_1 \\
&- 60qp_2 - 60p_1p_2 - 44m_\pi^2 + 58m_K^2) \\
&+ m_K^2(12q^2 + 24qp_1 \\
&+ 24qp_2 + 24p_1p_2 + 13m_K^2)]B(m_\pi^2,m_\eta^2,m_K^2) \\
&- \frac{1}{9(q^2+2qp_1+2qp_2)} \\
&\times [m_\pi^2(6q^2 + 12qp_1 + 12qp_2 + 39p_1p_2 \\
&+ 11m_\pi^2 + 4m_K^2 - 9m_\eta^2) - 9p_1p_2m_\eta^2] \\
&\times B_1(m_\pi^2,m_\eta^2,m_K^2) \\
&+ \frac{1}{2(q^2+2qp_1+2qp_2)} \\
&\times [m_\pi^2(2m_\pi^2 + 6p_1p_2 + 9m_K^2 - 6m_\eta^2) \\
&+ m_K^2(-2m_K^2 + 6p_1p_2 + 3m_\eta^2) - 6p_1p_2m_\eta^2] \\
&\times B_1(m_\pi^2,m_K^2,m_\eta^2) \\
&+ 3B_{00}(q^2,m_K^2,m_K^2) - 2B_{00}((p_1+q)^2,m_\eta^2,m_K^2) \\
&+ \frac{4(m_\pi^2+3p_1p_2)}{3(q^2+2qp_1+2qp_2)}B_{00}(m_\pi^2,m_\eta^2,m_K^2) \\
&+ 2B_{00}((p_1+q)^2,m_\eta^2,m_K^2) \\
&- \frac{2(2m_\pi^2+3p_1p_2)}{q^2+2qp_1+2qp_2}B_{00}(m_\pi^2,m_K^2,m_\eta^2) \\
&+ \frac{4m_\pi^2(m_\pi^2+3p_1p_2)}{3(q^2+2qp_1+2qp_2)}B_{11}(m_\pi^2,m_\eta^2,m_K^2) \\
&- \frac{2m_\pi^2(2m_\pi^2+3p_1p_2)}{q^2+2qp_1+2qp_2}B_{11}(m_\pi^2,m_K^2,m_\eta^2) \\
&+ 2(m_K^2-m_\pi^2)C_{00}(m_\pi^2,(p_1+q)^2,m_\eta^2,m_K^2)\Big\}. \qquad \text{(C.2)}
\end{aligned}
$$

The remaining contributions from $(K,\pi)$ pairs are collected in the form factors $\mathcal{F}_{16}^{+\mathrm{l}}$ and $\mathcal{F}_{26}^{+\mathrm{l}}$. The first parts refer to $(K^0,\pi^0)$ contributions, then $(\pi^0,K^-)$, $(K^0,\pi^-)$ and $(K^+,\pi^+)$ contributions are presented.

$$
\begin{aligned}
\mathcal{F}_{16}^{+\mathrm{l}} = \frac{-\mathrm{i}eG_8}{F}\Bigg\{ & \frac{1}{(q^2+2qp_1)(q^2+2qp_1+2qp_2)} \\
&\times \Bigg[-\frac{1}{2}(2m_\pi^2(2m_\pi^2 + q^2 + 2qp_1 + 2qp_2 + 4p_1p_2) \\
&+ m_K^2(-m_K^2 + q^2 + 2qp_1 - 2qp_2) \\
&+ 2p_1p_2(q^2 + 2qp_1 + 2qp_2 + 2p_1p_2))A(m_\pi^2) \\
&+ \frac{m_K^2}{2}(2m_\pi^2(2m_\pi^2 - 2m_K^2 + q^2 + 2qp_1 + 2p_1p_2) \\
&+ m_K^2(m_K^2 - q^2 - 2qp_1 - 2p_1p_2)) \\
&\times B(m_\pi^2,m_K^2,m_\pi^2) \\
&- (m_\pi^2m_K^2(-m_K^2 + 2m_\pi^2 + q^2 + 2qp_1 \\
&+ 4qp_2 + 6p_1p_2) \\
&- 2m_\pi^2p_1p_2(2m_\pi^2 + q^2 + 2qp_1 + 2qp_2 + 2p_1p_2) \\
&+ m_K^2p_1p_2(-m_K^2 + q^2 + 2qp_1 + 2qp_2 + 2p_1p_2) \\
&- 4m_\pi^4qp_2 - m_K^4qp_2)B_1(m_\pi^2,m_K^2,m_\pi^2) \\
&- 2(p_1p_2(2m_\pi^2 - m_K^2 + q^2 \\
&+ 2qp_1 + 2qp_2 + 2p_1p_2) \\
&+ 2m_\pi^2qp_2 - m_K^2qp_2) \\
&\times (B_{00}(m_\pi^2,m_K^2,m_\pi^2) + m_\pi^2B_{11}(m_\pi^2,m_K^2,m_\pi^2))\Bigg] \\
&+ \frac{1}{3(q^2+2qp_1)(q^2+2qp_1+2qp_2)} \\
&\times [2m_\pi^2(q^2 + 2qp_1 + 4qp_2) \\
&+ m_K^2(-q^2 - 2qp_1 + qp_2) \\
&+ 2q^2(q^2 + 4qp_1 + 4qp_2 + p_1p_2) \\
&+ 4p_1p_2(qp_1 + 2qp_2) \\
&+ 8(qp_1^2 + qp_2^2 + 2qp_1qp_2)]A(m_K^2)
\end{aligned}
$$

$$
\begin{aligned}
&- \frac{1}{3(d-1)} A(m_K^2) \\
&+ \frac{1}{6(d-1)} (q^2 - 4m_K^2) B(q^2, m_K^2, m_K^2) \\
&- \frac{1}{(q^2 + 2qp_1)(q^2 + 2qp_1 + 2qp_2)} \\
&\times [2m_\pi^2 (q^2 + 2qp_1 + 3qp_2) - m_K^2 (q^2 + 2qp_1) \\
&+ 2q^2 (q^2 + 4qp_1 + 4qp_2 + p_1p_2) \\
&+ 4p_1p_2 (qp_1 + 2qp_2) \\
&+ 8(qp_1^2 + qp_2^2 + 2qp_1qp_2)] A(m_\pi^2) \\
&+ \frac{1}{q^2 + 2qp_1 + 2qp_2} \\
&\times [-(q^2 (m_K^2 - m_\pi^2) - m_K^4 \\
&+ m_\pi^2 m_K^2 - 2m_\pi^2 (qp_1 + qp_2) \\
&+ 2m_K^2 (qp_1 + qp_2)) B(m_\pi^2, m_K^2, m_\pi^2) \\
&+ 2p_1p_2 (m_K^2 - m_\pi^2) B_1(m_\pi^2, m_K^2, m_\pi^2)] \\
&- \frac{1}{q^2 + 2qp_1} \\
&\times [(-2m_\pi^4 + 2m_\pi^2 m_K^2 - 2m_\pi^2 (qp_2 + p_1p_2) \\
&+ 2m_K^2 (qp_2 + p_1p_2)) B((p_1 + q)^2, m_K^2, m_\pi^2) \\
&+ 2(m_K^2 - m_\pi^2)(qp_2 + p_1p_2) \\
&\times B_1((p_1 + q)^2, m_K^2, m_\pi^2)] \\
&+ 2B_{00}(q^2, m_\pi^2, m_\pi^2) \\
&+ [2m_\pi^2 (m_\pi^2 - m_K^2 + qp_2 + p_1p_2) \\
&- 2m_K^2 (qp_2 + p_1p_2)] C(m_\pi^2, (p_1 + q)^2, m_K^2, m_\pi^2) \\
&- [2m_\pi^2 (m_\pi^2 - m_K^2 + qp_2) - 2m_K^2 qp_2] \\
&\times C_1(m_\pi^2, (p_1 + q)^2, m_K^2, m_\pi^2) \\
&- 2m_\pi^2 (m_\pi^2 - m_K^2) C_2(m_\pi^2, (p_1 + q)^2, m_K^2, m_\pi^2) \\
&- 2p_1p_2 (m_\pi^2 - m_K^2) C_{11}(m_\pi^2, (p_1 + q)^2, m_K^2, m_\pi^2) \\
&- 2(m_\pi^2 - m_K^2)(qp_2 + p_1p_2) \\
&\times C_{22}(m_\pi^2, (p_1 + q)^2, m_K^2, m_\pi^2) \\
&- 2(m_\pi^2 - m_K^2)(qp_2 + 2p_1p_2) \\
&\times C_{12}(m_\pi^2, (p_1 + q)^2, m_K^2, m_\pi^2) \\
&+ \frac{1}{3(q^2 + 2qp_1)(q^2 + 2qp_1 + 2qp_2)} \\
&\times [-(2m_\pi^2 (4m_\pi^2 - 4m_K^2 - q^2 \\
&- 2qp_1 + 8qp_2 + 12p_1p_2) \\
&+ m_K^2 (2m_K^2 + q^2 + 2qp_1 - 8qp_2 - 12p_1p_2) \\
&+ 2p_1p_2 (q^2 + 2qp_1 + 8qp_2 + 8p_1p_2)) A(m_\pi^2) \\
&- m_K^2 (2m_\pi^2 (2m_\pi^2 - 3m_K^2 - 2q^2 \\
&- 4qp_1 + 2qp_2 + 4p_1p_2) \\
&+ m_K^2 (2m_K^2 + q^2 + 2qp_1 - 2qp_2 - 6p_1p_2) \\
&+ 4p_1p_2 (-q^2 - 2qp_1 + qp_2 + p_1p_2)) \\
&\times B(m_\pi^2, m_K^2, m_\pi^2) \\
&+ 2(4m_\pi^6 + 4m_\pi^4 (-2m_K^2 - q^2 - 2qp_1 + qp_2 + 2p_1p_2) \\
&+ 3m_K^4 (m_\pi^2 + qp_2 + p_1p_2) \\
&+ 2m_\pi^2 p_1p_2 (-7m_K^2 - 2q^2 - 4qp_1 + 2qp_2 + 2p_1p_2) \\
&- 3m_K^2 p_1p_2 (q^2 + 2qp_1 + 2qp_2 + 2p_1p_2) \\
&- 8m_\pi^2 m_K^2 qp_2) B_1(m_\pi^2, m_K^2, m_\pi^2) \\
&+ 4(m_\pi^2 (2m_\pi^2 - m_K^2 + q^2 + 2qp_1 + 6qp_2 + 8p_1p_2) \\
&- 3m_K^2 (qp_2 + p_1p_2) \\
&+ 3p_1p_2 (q^2 + 2qp_1 + 2qp_2 + 2p_1p_2)) \\
&\times (B_{00}(m_\pi^2, m_K^2, m_\pi^2) \\
&+ m_\pi^2 \; B_{11}(m_\pi^2, m_K^2, m_\pi^2))] + 2B_{00}(q^2, m_K^2, m_K^2) \Big\} .
\end{aligned}
\tag{C.3}
$$

$\mathcal{F}_{26}^{+\mathrm{l}}$ is organized in the same way and reads as follows:

$$
\begin{aligned}
\mathcal{F}_{26}^{+\mathrm{l}} = \frac{-\mathrm{i}eG_8}{F} \Big\{ & \frac{1}{q^2 + 2qp_1 + 2qp_2} \\
&\times \Big[ \frac{1}{2} (2m_\pi^2 - 3m_K^2 + 2p_1p_2) A(m_\pi^2) \\
&+ \frac{m_K^2}{2} (2m_\pi^2 - m_K^2) B(m_\pi^2, m_K^2, m_\pi^2) \\
&- (2m_\pi^4 + m_K^4 - 2m_\pi^2 m_K^2 - m_K^2 p_1p_2) \\
&\times B_1(m_\pi^2, m_K^2, m_\pi^2) \\
&- 2p_1p_2 (B_{00}(m_\pi^2, m_K^2, m_\pi^2) + m_\pi^2 \\
&\times \; B_{11}(m_\pi^2, m_K^2, m_\pi^2))] \\
&+ \frac{1}{6(q^2 + 2qp_1 + 2qp_2)} \\
&\times [-4m_\pi^2 - 3m_K^2 + q^2 + 2qp_1 + 2qp_2 - 4p_1p_2] \\
&\times A(m_K^2) \\
&- \frac{1}{2(d-1)} A(m_K^2) \\
&+ \frac{1}{4(d-1)} (q^2 - 4m_K^2) B(q^2, m_K^2, m_K^2) \\
&+ \frac{1}{q^2 + 2qp_1 + 2qp_2} \\
&\times [(m_\pi^2 + m_K^2 + 2p_1p_2) A(m_\pi^2) \\
&+ m_K^2 (m_K^2 - m_\pi^2) B(m_\pi^2, m_K^2, m_\pi^2) \\
&+ 2p_1p_2 (m_K^2 - m_\pi^2) B_1(m_\pi^2, m_K^2, m_\pi^2)] \\
&+ 2B_{00}(q^2, m_\pi^2, m_\pi^2) \\
&+ 2(m_K^2 - m_\pi^2) C_{00}(m_\pi^2, (p_1 + q)^2, m_K^2, m_\pi^2) \\
&+ \frac{1}{3(q^2 + 2qp_1 + 2qp_2)} \\
&\times [4(2m_\pi^2 - m_K^2 + p_1p_2) A(m_\pi^2) \\
&+ 2m_K^2 (m_\pi^2 + p_1p_2) B(m_\pi^2, m_K^2, m_\pi^2) \\
&- 2[m_\pi^2 (2m_\pi^2 - 3m_K^2 + 2p_1p_2) \\
&+ m_K^2 (2m_K^2 - p_1p_2)] B_1(m_\pi^2, m_K^2, m_\pi^2)] \\
&+ \frac{2}{3} [(m_\pi^2 - m_K^2 + qp_1 + p_1p_2) \\
&\times B((p_2 + q)^2, m_K^2, m_\pi^2) \\
&+ (m_K^2 + q^2 + 2qp_1 + 2qp_2 + 2p_1p_2) \\
&\times B_1((p_2 + q)^2, m_K^2, m_\pi^2)] \\
&- \frac{4(3m_\pi^2 - 2m_K^2 + p_1p_2)}{3(q^2 + 2qp_1 + 2qp_2)} \\
&\times [B_{00}(m_\pi^2, m_K^2, m_\pi^2) + m_\pi^2 B_{11}(m_\pi^2, m_K^2, m_\pi^2)]
\end{aligned}
$$

$$
\begin{aligned}
&- \frac{1}{3}[(2m_\pi^2 - 3m_K^2 + 2qp_1 + 2p_1p_2)B(q^2, m_\pi^2, m_\pi^2) \\
&+ (3m_K^2 + 2q^2 + 4qp_1 + 4qp_2 + 4p_1p_2) \\
&\times B_1((p_2+q)^2, m_K^2, m_\pi^2)] \\
&- \frac{2}{3}m_K^2(m_\pi^2 - m_K^2 + qp_1 + p_1p_2) \\
&\times C(m_\pi^2, (p_2+q)^2, m_K^2, m_\pi^2) \\
&+ \frac{1}{3}[4m_\pi^2(m_\pi^2 - m_K^2 + qp_1 + p_1p_2) + m_K^4] \\
&\times C_1(m_\pi^2, (p_2+q)^2, m_K^2, m_\pi^2) \\
&+ \frac{1}{3}[4m_\pi^2(m_\pi^2 - m_K^2 + qp_1 + qp_2 + p_1p_2) \\
&+ 4qp_2(-m_K^2 + qp_1 + p_1p_2) + m_K^4] \\
&\times C_2(m_\pi^2, (p_2+q)^2, m_K^2, m_\pi^2) \\
&- \frac{2}{3}m_K^2[C_{00}(m_\pi^2, (p_2+q)^2, m_K^2, m_\pi^2) \\
&+ m_\pi^2 C_{11}(m_\pi^2, (p_2+q)^2, m_K^2, m_\pi^2) \\
&+ (m_\pi^2 + qp_2)C_{22}(m_\pi^2, (p_2+q)^2, m_K^2, m_\pi^2) \\
&+ (2m_\pi^2 + qp_2)C_{12}(m_\pi^2, (p_2+q)^2, m_K^2, m_\pi^2)] \\
&+ \frac{2}{3}B_{00}(q^2, m_K^2, m_K^2)\Big\}. \qquad \text{(C.4)}
\end{aligned}
$$

## References


1. L.M. Sehgal, M. Wanninger, Phys. Rev. D **46**, 1035 (1992); ibid. D **46**, 5209(E) (1992)
2. P. Heiliger, L.M. Sehgal, Phys. Rev. D **48**, 4146 (1993); ibid D **60**, 079902(E) (1999)
3. J.K. Elwood, M.J. Savage, M.B. Wise, Phys. Rev. D **52**, 5095 (1995); ibid. D **53**, 2855(E) (1996)
4. M.J. Savage, hep-ph/9908324
5. J. Adams et al. (KTeV Collaboration), Phys. Rev. Lett. **80**, 4123 (1998)
6. Y. Takeuchi et al., Phys. Lett. B **443**, 409 (1998)
7. E. Mazzucato (NA48 Collaboration), talk presented at the International Conference on $CP$ Violation Physics, 18–22 September 2000, Ferrara, Italy
8. A. Bizzeti (NA48 Collaboration), hep-ex/0102035
9. J.K. Elwood, M.J. Savage, J.W. Walden, M.B. Wise, Phys. Rev. D **53**, 4078 (1996)
10. G. Ecker, H. Pichl, hep-ph/0101097
11. A. Alavi-Harati et al. (KTeV Collaboration), Phys. Rev. Lett. **84**, 408 (2000)
12. J. Belz (KTeV Collaboration), hep-ex/9903025
13. J. van Leusen, L.M. Sehgal, Phys. Rev. Lett. **83**, 4933 (1999)
14. J. van Leusen, L.M. Sehgal, Phys. Lett. B **489**, 300 (2000)
15. T. Barker (KTeV Collaboration), JHEP Proceedings, Heavy Flavours 8, Southampton, UK, 1999
16. A.R. Barker, S.H. Kettell, Ann. Rev. Nucl. Part. Sci. **50**, 249 (2000)
17. S. Adler et al. (E787 Collaboration), Phys. Rev. Lett. **85**, 4856 (2000)
18. J. Gasser, H. Leutwyler, Ann. Phys. **158**, 142 (1984)
19. J. Gasser, H. Leutwyler, Nucl. Phys. B **250**, 465 (1985)
20. J. Kambor, J. Missimer, D. Wyler, Phys. Lett. B **261**, 496 (1991)
21. J. Kambor, J. Missimer, D. Wyler, Nucl. Phys. B **346**, 17 (1990)
22. G. Ecker, J. Kambor, D. Wyler, Nucl. Phys. B **394**, 101 (1993)
23. G. Ecker, H. Neufeld, A. Pich, Phys. Lett. B **278**, 337 (1992)
24. J. Bijnens, G. Ecker, A. Pich, Phys. Lett. B **286**, 341 (1992)
25. G. Ecker, H. Neufeld, A. Pich, Nucl. Phys. B **413**, 321 (1994)
26. E.J. Ramberg et al., Phys. Rev. Lett. **70**, 2525 (1993)
27. G. Ecker, A. Pich, E. de Rafael, Nucl. Phys. B **291**, 692 (1987)
28. C. Alliegro et al., Phys. Rev. Lett. **68**, 278 (1992)
29. G. D'Ambrosio, G. Ecker, G. Isidori, J. Portolés, JHEP **8**, 4 (1998)
30. R. Appel et al., (E865 Collaboration), Phys. Rev. Lett. **83**, 4482 (1999)
31. R. Funck, J. Kambor, Nucl. Phys. B **396**, 53 (1993)
32. S.D. Ellis, R. Kleiss, W.J. Stirling, Comp. Phys. Comm. **40**, 359 (1986)
33. C. Bruno, J. Prades, Z. Phys. C **57**, 585 (1993)
34. G. D'Ambrosio, J. Portolés, Nucl. Phys. B **492**, 417 (1997)
35. G. D'Ambrosio, J. Portolés, Nucl. Phys. B **533**, 494 (1998)